

Site selection for municipal solid waste landfills in arid regions based on fuzzy decision-making—A Case Study in the Hexi Corridor of China

Jiamin Liu

Lanzhou University

Bin Xiao

Lanzhou University

Yueshi Li

Lanzhou University

Xiaoyun Wang

Lanzhou University

Jizong Jiao (✉ Jiaojz@lzu.edu.cn)

Lanzhou University

Jian Bi

Lanzhou University

Research Article

Keywords: FAHP, MSW, Landfill site selection, Hexi corridor, Group fuzzy MULTIMOORA

Posted Date: March 29th, 2021

DOI: <https://doi.org/10.21203/rs.3.rs-305236/v1>

License: © ⓘ This work is licensed under a Creative Commons Attribution 4.0 International License.

[Read Full License](#)

1 Site selection for municipal solid waste landfills in arid regions based on
2 fuzzy decision-making: A Case Study in the Hexi Corridor of China

3 Jiamin Liu^{1,2}, Bin Xiao^{1,2}, Yueshi Li^{1,2}, Xiaoyun Wang^{1,2}, Jizong Jiao^{1,2,*}, Jian Bi^{1,2}

4 1. College of Earth and Environment Sciences, Lanzhou University, Lanzhou
5 730000, China.

6 2. The Key Laboratory of Western China's Environmental Systems, Ministry of
7 Education (MOE), Lanzhou 730000, China

8 **Abstract:** The rational and scientific selection of Municipal Solid Waste (MSW)
9 landfill sites is becoming increasingly important, due to the continuous growth of MSW
10 worldwide. Multi-source information is employed to ensure the accuracy of the
11 evaluation criteria, including hydrogeological, morphological, environmental, climatic
12 and socio-economic data. In the fuzzy logic environment, a Fuzzy Analytic Hierarchy
13 Process (FAHP) and GIS spatial technique have been utilized to locate potential landfill
14 sites. Landfill Site Selection Results (LSSR) were divided into three categories: suitable,
15 less suitable, and unsuitable. Suitable areas were further divided into high, moderate,
16 and low levels. We used the field investigations of 28 standardized landfill sites in the
17 Hexi Corridor of China that comply with the China National Standard (CNS) to verify
18 the LSSR. These sites are then ranked utilizing group fuzzy MULTIMOORA. These
19 methods were more feasible and accurate in assessing the suitability of MSW landfills.
20 The highlights of our methods were as follows: (1) The uncertainty of AHP expert

21 scoring reduced by employing the fuzzy membership function, and the decision
22 efficiency of spatial analysis improved as well. (2) Verification results showed that the
23 main LSSR met the CNS perfectly and located suitable areas, with an accuracy of 93%
24 (26 out of 28 sites). (3) In the highly suitable areas, 11 candidate areas were selected
25 for the MSW landfill site construction in the Hexi Corridor. Furthermore, technical
26 countermeasures for the standardized management of MSW landfills were proposed for
27 the Hexi Corridor, which is critical for ecological/environmental protection.

28 **Keywords:**

29 FAHP

30 MSW

31 Landfill site selection

32 Hexi corridor

33 Group fuzzy MULTIMOORA

34

35 *Corresponding author. E-mail: jiaojz@lzu.edu.cn (J. Jiao).

36

37 **Declaration**

38 **Funding:** This work was supported by [the National Key R&D Program of China]

39 (Grant numbers [2018YFC1903700]).

40 **Conflicts of interest/Competing interests:** The authors declare that they have no
41 known competing financial interests or personal relationships that could have appeared
42 to influence the work reported in this paper.

43 **Ethics approval:** All authors have read this manuscript and would like to have it
44 considered exclusively for publication in **ENVIRONMENTAL SCIENCE AND**
45 **POLLUTION RESEARCH.** None of the material related to this manuscript has been
46 published or is under consideration for publication elsewhere, including the internet.
47 These articles report original research with broad scientific significance and importance.
48 Consequently, this article is Research Articles.

49 **Consent to participate** All authors have read this manuscript and would like to
50 have it considered exclusively for publication in **ENVIRONMENTAL SCIENCE**
51 **AND POLLUTION RESEARCH.**

52 **Consent for publication:** After Acceptance, we will either grant the Publisher an
53 exclusive licence to publish the article or will be asked to transfer copyright of the
54 article to the Publisher.

55 **Availability of data and material:** Agree with transparent.

56 **Code availability:** Agree with transparent.

57 **Authors' contributions:** Data curation: [JiaMin Liu]; Software: [JiaMin Liu];
58 Formal analysis: [JiaMin Liu]; Visualization: [JiaMin Liu]; Writing - original draft:
59 [JiaMin Liu]; Methodology: [Bin Xiao]; Resources: [Bin Xiao]; Writing - review &

60 editing: [Yueshi Li, Jizong Jiao]; Supervision: [Jizong Jiao, Xiaoyun Wang];
61 Conceptualization: [Jizong Jiao, Jian Bi]; Validation: [Jizong Jiao, Xiaoyun Wang];
62 Funding acquisition: [Jizong Jiao].

63

64 **Acknowledgments:** We would like to thank the data providers, authors and
65 funders.

66

67 **1. Introduction**

68 While urbanization promotes higher anthropogenic living standards, it also creates
69 a series of significant challenges, such as increased waste production (Hoo et al., 2018);
70 thus, the management of MSW is of great concern on a global scale (Turcott Cervantes
71 et al., 2018). According to Chinese statistics, the annual growth rate ranges from
72 8%~11.5%, where 2/3 of cities are surrounded by MSW sites (Luo et al., 2018), which
73 can hinder economic development to a certain extent (Liu et al., 2014).

74 The composition of MSW is complex and is typically separated by domestic waste,
75 industrial solid waste, agricultural solid waste, and other waste (Han et al., 2019).
76 Although China has experimented with waste classification and harmless treatment
77 policies in Shanghai and other developed cities since 2018, landfills remain the most
78 important and efficacious means for the disposal of most MSW (Zhang et al., 2019).
79 Over time, the leachate produced by chemical degradation in landfills tend to

80 contaminate surface water and groundwater (Calabro et al., 2018). Further, the ambient
81 atmosphere, soil, and water are contaminated by microbial decomposition releases of
82 NH_3 , H_2S , and harmful hydrocarbon gases (Peng et al., 2018). Meanwhile, landfills
83 require large tracts of land; thus, existing landfills in most areas of China cannot meet
84 the ever-growing demand for MSW. Consequently, it is imperative that the locations of
85 landfill sites be prudently selected based on the best science and rationale (Kamdar et
86 al., 2019).

87 In recent years, a variety of Multi-Criteria Decision Analysis (MCDA) methods
88 have been employed for the Landfill Site Selection (LSS) research (Davami et al., 2014),
89 encompassing the Analytic Hierarchy Process (Asefi et al.) (Torabi-Kaveh et al., 2016),
90 Fuzzy Analytic Hierarchy Process (FAHP) (Hanine et al., 2016), Preference Ranking
91 Organization Method (PROMETHEE) (Hamzeh et al., 2015), Analysis Network
92 Process (ANP) (Bahrani et al., 2016), Technique for Order Preference by Similarity to
93 Ideal Solution (TOPSIS) (Asefi and Lim, 2017), and Fuzzy TOPSIS (Beskese et al.,
94 2015).

95 Integrated MCDA and GIS are the more commonly used models for LSS. AHP
96 utilizes relative importance to compare qualitative and quantitative criteria, which can
97 minimize the inconsistency of judgments (Torabi-Kaveh et al., 2016). Fuzzy logic
98 provides a broad set of fuzzy membership functions, including linear, triangular,
99 trapezoidal, Sigmoidal, Gaussian and Gamma functions (Al-Ruzouq et al., 2018).
100 FAHP introduces fuzzy logic on the basis of AHP to resolve complex multi-criteria/

101 multi-level decision-making challenges (Rezaeisabzevar et al., 2020). The emergence
102 of massive quantities of data has enabled modeling research and analysis based on
103 spatial data and other tools, where the application of GIS has become commonplace
104 (Afzali et al., 2014).

105 Fuzzy membership functions and GIS tools have been widely employed in LSS
106 (Spigolon et al., 2018) , and several researchers used 13 evaluation criteria and a
107 triangular fuzzy membership function to select optimal landfill sites (Karimi et al.,
108 2020). Other researchers utilized 10 criteria and fuzzy logic space modeling methods
109 to identify landfills (Soroudi et al., 2018). However, a few studies in the literature
110 describe the combination of more than 20 evaluation criteria with multiple fuzzy
111 membership functions. The adoption of multiple sets of fuzzy membership functions
112 for scenario simulation can better transform the logical relation of criterion attributes
113 to membership degree, effectively reducing the uncertainty of decision-making
114 (Eskandari et al., 2016). As relates verifications, nighttime satellite imagery and
115 sensitivity analysis have been exploited to verify the LSSR (Karimi et al., 2020).
116 However, no reports to date have employed existing standard landfill locations to verify
117 the LSSR. In addition, we discuss several Fuzzy MULTIMOORA tools for ranking to
118 produce the final rankings and clarifying the robustness of the MCDA method.

119 The Hexi Corridor comprises one of the most arid areas in China (Huang et al.,
120 2017). The ecological environment is extremely fragile, with a poor anti-interference
121 capacity, and is one of the strategic regions for environmental development and

122 protection in Northwest China (Williams et al., 2009). Nevertheless, existing research
123 has concentrated primarily on the LSS in humid areas, and few reports exist on the
124 study of arid areas with fragile ecological environments (Osra and Kajjumba, 2020).
125 Therefore, it is of particular importance to scientifically and rationally select landfill
126 sites for MSW that minimize negative environmental impacts (Uyan, 2014).

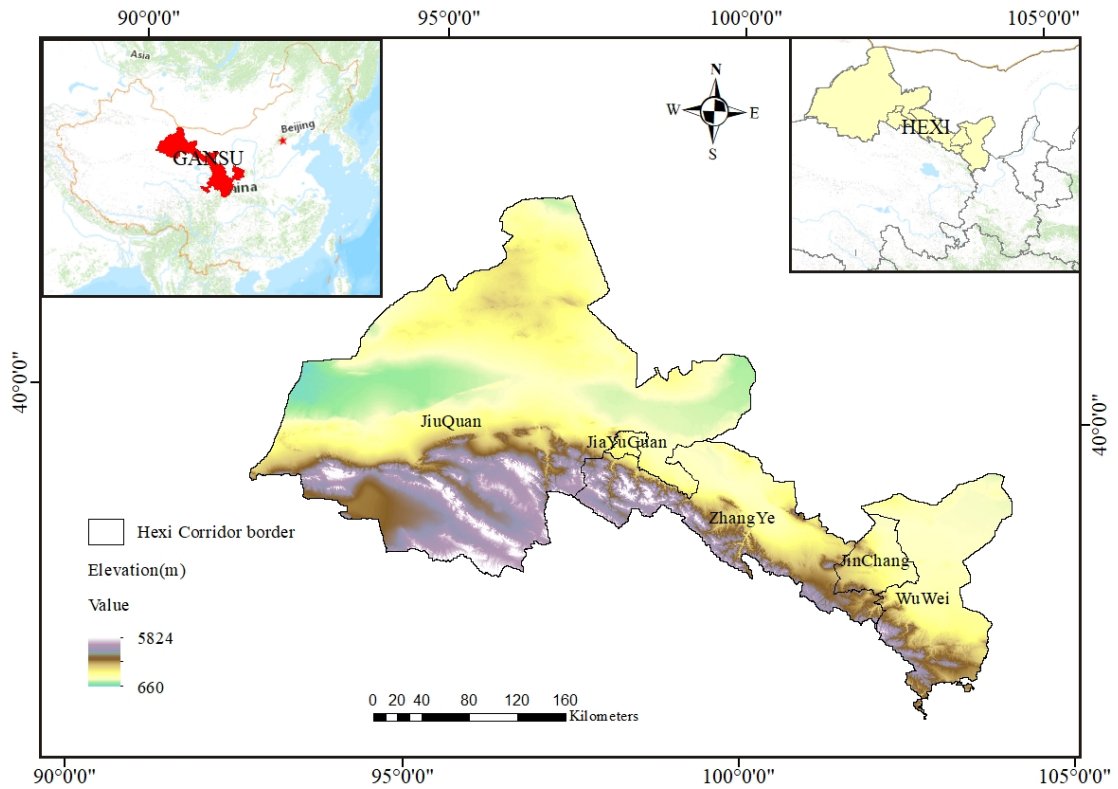
127 To encapsulate, taking the Hexi Corridor in China as a case study, we endeavored
128 to integrate FAHP-GIS methods, select 20 valuation criteria, and determine multiple
129 fuzzy membership functions, toward the identification of new suitable and scientifically
130 vetted landfill areas. The LSSR was employed to provide reliable and technological
131 support for the scientific management of solid waste in this region, while guiding
132 effective urban planning.

133 **2. Materials and methods**

134 2.1. Study area

135 The Hexi Corridor (**Fig. 1**) is located in the northwest of Gansu Province, China
136 ($93^{\circ}20'E$ — $104^{\circ}00'E$, $37^{\circ}10'N$ — $42^{\circ}50'N$) (Zhang et al., 2016). The improper disposal
137 of MSW is one of the most important factors leading to increasingly serious
138 environmental pollution in this area (Huang et al., 2017). According to statistics from
139 the Gansu Environmental Statistics Bulletin (GESB, 2009), it was estimated that the
140 Hexi Corridor generated 0.6825 million tons of domestic waste, 19.2056 million tons
141 of industrial solid waste and 1.6031 million tons of agricultural solid waste annually. In

142 2018, the Hexi Corridor produced 1.1894 million tons of domestic waste, 43. 2496
143 million tons of industrial solid waste, and 2.6082 million tons of agricultural solid waste.



144 90°0'0" 95°0'0" 100°0'0" 105°0'0"

145 **Fig. 1.** Elevation of the study region. The Hexi Corridor includes five cities (Jiuquan, Jiayuguan,
146 Zhangye, Jinchang, Wuwei), and twenty counties (districts), with a total area of 2.7×10^5 km².
147 Elevation data is from the USGS - SRTM dataset, which provides elevation data at a 30-meter
148 resolution. The elevation of the study area ranged from 660 to 5842 meters.

149 2.2. Data collection

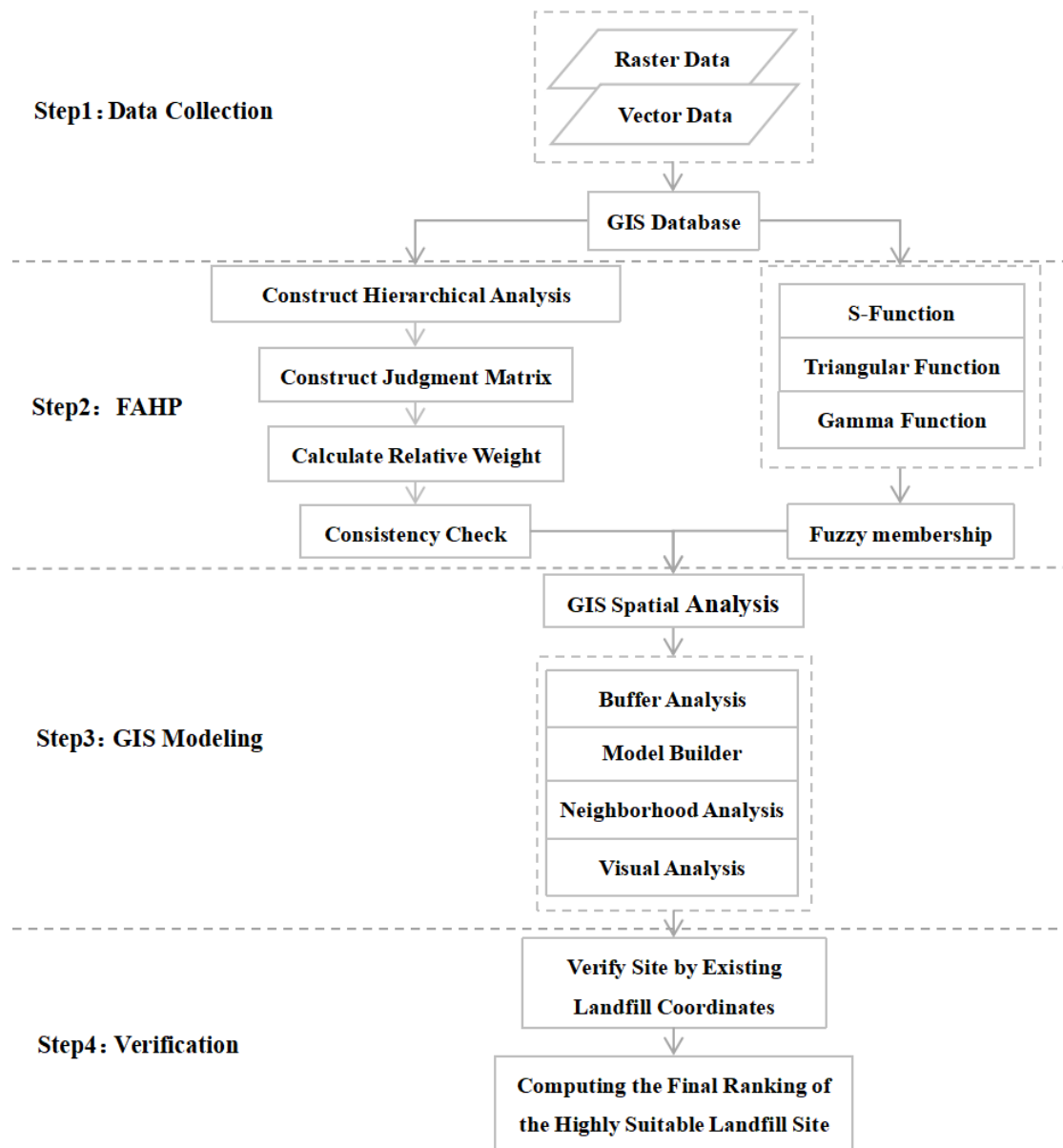
150 Source data for groundwater depth and quality was provided by the Gansu Water
151 Resources Department (GWRD, 2019). The groundwater richness content and faults
152 source data were obtained from the Gansu Bureau of Geology and Mineral
153 Hydrogeology Engineering Geological Exploration Institute (GBGMHEGEI, 2015).

154 Earthquake related data was accessed from the Gansu Earthquake Agency online portal
155 (GEA, 2015). Normalized vegetation index (NDVI) of MOD13Q1 products was
156 derived from the online MODIS data website (MODIS, 2018). We obtained surface
157 water, settlements and roads data from the National Catalogue Service for Geographic
158 Information (NCSGI, 2015). Ecological function reserves data was obtained from the
159 Gansu Forestry and Grass Bureau (GFGB, 2015). Shuttle Radar Topography Mission
160 (SRTM) digital data were obtained from the online website of USGS Earth Explorer,
161 with a spatial resolution of 30m (USGS, 2015). The landform, soil, and 30m land use
162 types, as well as temperature, precipitation meteorological, economic, population,
163 administrative division and basic geographic space data were acquired from the
164 Resource and Environmental Science and Data Center, Chinese Academy of Sciences
165 (RESDC, 2015). All of the criterion data sets used in this study, as well as their formats
166 and sources are described in **Table A1** in Appendix A.

167 2.3. Method framework

168 We describe the specific process employed for this study inclusive of multi-source
169 data collection and preprocessing in **Fig. 2**: (1) Groundwater depth and quality data
170 were interpolated via the kriging interpolation method, whereas the vector point,
171 polyline, and polygon data were converted to raster data, imported into the GIS spatial
172 database and unified spatial reference in the WGS_Albers_System projection
173 coordinate system. (2) FAHP was employed to establish an evaluation criteria system
174 and obtain the weight of evaluation criteria, construct a judgment matrix, check for

175 consistency, as well as to set up membership functions of the S-function, Triangular
176 function, and Gamma function. (3) GIS spatial analysis and modeling involved the
177 establishment of buffer zones for faults, earthquake points, surface water, settlements,
178 roads, and ecological function reserve evaluation criteria. The model builder in ArcGIS
179 was used for modeling to achieve a weighted overlay of layers and neighborhood
180 smoothing, to obtain the results of landfill site selection through GIS visualization. (4)
181 The LSSR were verified by the coordinates of the landfill sites that conformed to the
182 CNS, these sites are then ranked utilizing group fuzzy MULTIMOORA.



183

184 **Fig. 2.** Method framework chart including the four main steps: Data Collection, FAHP, GIS
 185 Modeling, and Verification.

186 2.4. Criteria selection

187 The extraction of reasonable evaluation criteria determines the appropriateness
 188 and reliability of LSSR (De Feo and De Gisi, 2014). After discussing with authoritative
 189 professors and experts and referring to the relevant literature in strict accordance with

190 the CNS, the selected qualitative and quantitative evaluation criteria (C₁, C₂, C₃,
191 C₄.....C₂₀) for landfill sites were established. Since LSS is a complex task in MSW,
192 one should consider hydrogeological, morphological, environmental, climatic, and
193 socio-economic factors for the overall situation (Soltani et al., 2015).

194 Hydrogeological aspects should be considered to avoid potential groundwater
195 contamination caused by the leakage of landfill leachate, while ensuring the safety of
196 construction and operation (Karakus et al., 2020). Morphological aspects were taken
197 into account to reduce construction costs and increase stability during
198 construction(Bahrani et al., 2016). Environmental aspects were taken into consideration
199 to minimize impacts on surrounding residents, and land/water resources (Ozkan et al.,
200 2019). Climatic issues were reviewed to reduce potential threats and damage to the
201 surrounding environment posed by various pollutants released from the landfill through
202 leachate or waste gas (Lima et al., 2018). Socio-economic impacts were considered to
203 prevent the landfill from adversely affecting the surrounding ecological reserves and
204 regional economic development (Asefi et al., 2020a). Further detailed information on
205 the criteria selection is contained **in Table B1** in Appendix B. The interval from 0 to 1
206 was adopted for normalization, where the larger the value, the better the suitability (**Fig.**
207 **C1, C2, C3, C4, and C5** in Appendix C).

208 The specific CNS for reference include: "Standard for Pollution Control on the
209 Landfill Site of Domestic Waste" (GB16889-2008), "Technical Specifications for
210 Sanitary Landfill of Domestic Waste" (GB50869-2013), "Standard for Pollution on the

211 Storage and Disposal Site for General Industrial Solid Waste" (GB18599-2001), "Water
212 Pollution Prevention Law of the People's Republic of China", "Regulations of the
213 People's Republic of China on Nature Reserves, " Technical Regulations for
214 Investigation of Land Use Status", and " Urban and Rural Planning Law of the People's
215 Republic of China". All CNS are available at the National Standard Full Text Open
216 System (NSFTOS, 2017).

217 2.4.1. Hydrogeological factors

218 The contamination of groundwater from landfills is dependent on the groundwater
219 depth and the permeability of the aquifers, with shallower groundwater being more
220 likely to be polluted. Consequently, landfills should developed at locations with
221 sufficient groundwater depth (Rezaeisabzevar et al., 2020). Groundwater quality is an
222 important factor that affects the LSSR (Przydatek and Kanownik, 2019) (refer to the
223 comprehensive evaluation method in "Groundwater Quality Standard" GB/T 14848-
224 2017). Contingent on the composition of its chemical components, groundwater quality
225 is separated into five categories, from high to low. The suitability of groundwater
226 quality was divided according to the actual situation of the study area. The more water-
227 rich the groundwater aquifer, the more difficult it is to build landfills and the higher the
228 cost (Sener et al., 2011). According to the actual status of the study area, the water
229 inflow from a single well classified the suitability of groundwater richness. The
230 establishment of landfills should be avoided in areas with active geological structures
231 or other underground terrain (Yousefi et al., 2018). As the permeability of rocks in

232 geological faults and earthquake zones increases, the resulting leachate may
233 contaminate groundwater (Eskandari et al., 2012). **Table B1** in Appendix B displays
234 the classification of groundwater depth, groundwater quality, groundwater richness,
235 distance from faults, and earthquake points. Normalized suitability maps are shown in
236 **Fig. C1** in Appendix C.

237 2.4.2. Morphological factors

238 The greater the elevation and slope, the more difficult it is to carry out the main
239 body and auxiliary projects of the landfill, and the higher the construction costs
240 (Motlagh and Sayadi, 2015). The terrain of the study area contained a complex and
241 diverse topography, with lower elevations considered to have reduced construction
242 costs. We combined the above conditions to assess the suitability of elevation and slope.
243 The basin landform is surrounded by mountains on three sides and with "S" or "Y"
244 gullies extending in the open direction, which is conducive to reducing pollution risks,
245 providing sufficient space, while extending landfill service and resource utilization
246 (Sureshkumar et al., 2017). The bottom of the basin or valley is gentle and wide, and
247 the landfill space is sufficient, which is conducive to extending the landfill service
248 (Sureshkumar et al., 2017). For the LSSR, the reduction of excessive damage to surface
249 vegetation should be considered (Kara and Doratli, 2012). In the study area, the
250 vegetation distribution is affected by natural factors such as climate, soil, hydrology,
251 and landform, showing obvious meridional and vertical zonal distribution. Considering
252 the impacts of different soil types on landfills, we classified soil type suitability. **Table**

253 **B1** in Appendix B shows the classification of elevation, slope, landform type, NDVI,
254 and soil type suitability, and got its normalized suitability map (**Fig. C2**, Appendix C).

255 2.4.3. Environmental factors

256 Landfills should not be located near ambient surface water such as ponds, lakes,
257 rivers, and streams to avoid their contamination (Torabi-Kaveh et al., 2016). In the
258 study area, the water all originates from the Qilian Mountains; thus, landfill sites
259 should be built downstream of the water source area as far as possible. Based on the
260 above situation, we assessed the suitability of surface water. Land use type directly
261 reflects the anthropogenic utilization of land and natural environment, as well as the
262 current status of land use on the surface, which provides a powerful basis for decision-
263 making in LSS planning (Motlagh and Sayadi, 2015). We classified the suitability of
264 land use types according to the available value of the study area. The development of
265 landfills is likely to initiate social conflicts and the "neighbor effect", as well as various
266 environmental problems (Khan et al., 2018). In the study area, the settlements were
267 concentrated in the oasis area of the corridor plain, with sufficient water resources,
268 convenient transportation, and high population carrying capacity. The LSS must also
269 consider road requirements, where the closer to the roads, the more convenient the
270 transportation conditions and the lower the cost of waste transfer (Ersoy et al., 2013).
271 **Table B1** in Appendix B reveals the division of the suitability of surface water, land
272 use type, settlements, and roads, whereas a normalized suitability map is shown in **Fig.**
273 **C3** in Appendix C.

274 2.4.4. Climatic factors

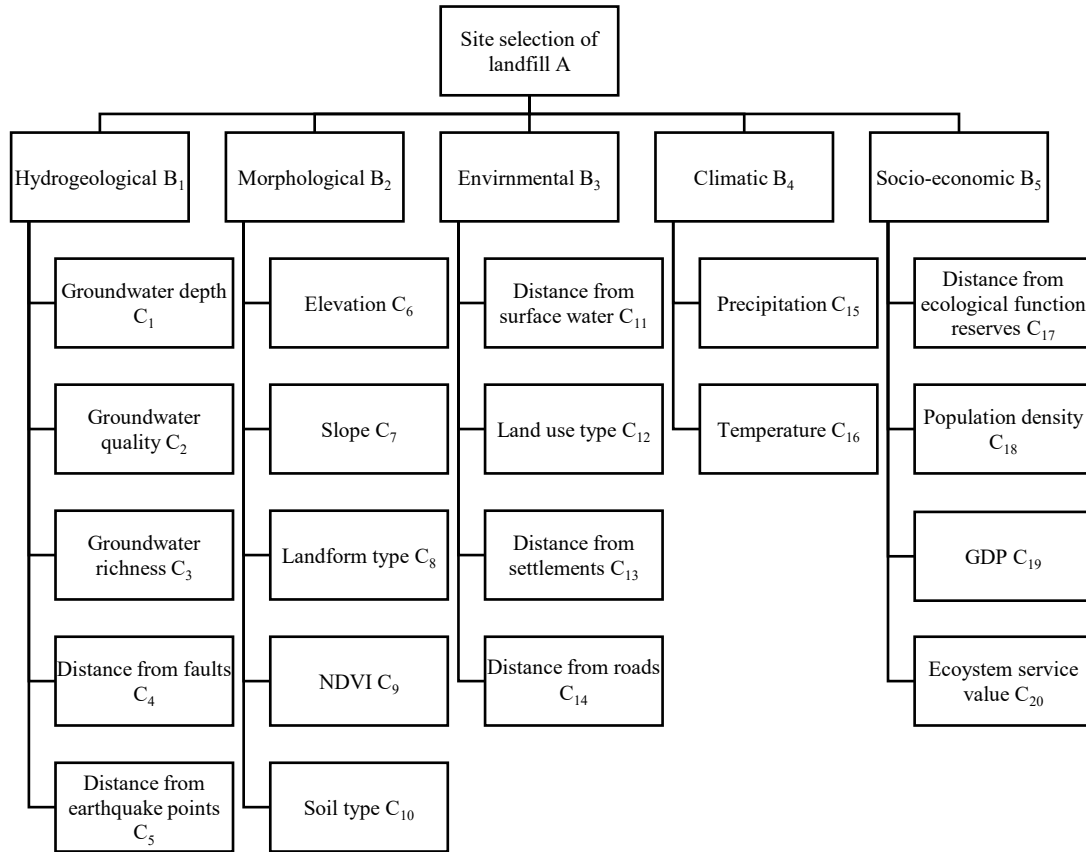
275 Precipitation and temperature are critical factors in the LSS process (Aksoy and
276 San, 2016). Areas with less precipitation and mild temperatures are more suitable for
277 construction landfills. Our study area belonged to a typical continental arid climate,
278 with a complex precipitation distribution and an average temperature of $\sim 7.06^{\circ}\text{C}$. The
279 suitability of precipitation and temperature were segregated according to the above
280 conditions (**Table B1** in Appendix B) to obtain a normalized suitability map (**Fig. C4**,
281 Appendix C).

282 2.4.5. Socio-economic factors

283 Ambient ecological function reserves primarily include entities that require
284 protection such as natural ecosystems, rare/endangered wild animal and plant species,
285 and natural relics of special significance. It is always the least desirable option to
286 develop landfills in close proximity to natural reserves (Sener et al., 2010). Concomitant
287 with higher population densities is more extensive urbanization (Farahbakhsh and
288 Forghani, 2019). Further, the higher the GDP in a given location, the higher its
289 economic level and the higher the added value of land will be (Aracil et al., 2018).
290 Indirect ecosystem service values reflect the value of land use, while the suitability of
291 landfills gradually decreases with higher ecosystem service values (Alavi et al., 2013).
292 We classified the ecological function reserves, population density, GDP, and ecosystem
293 service value suitability according to the status quo of the study area (**Table B1** in
294 Appendix B) to obtain a normalized suitability map (**Fig. C5** in Appendix C).

295 2.5. FAHP Model

296 A hierarchical analysis structure was constructed by selecting reasonable criteria
 297 and sub-criteria (Fig. 3).



298

299 **Fig. 3.** The hierarchical analysis structure is comprised of three layers (decision, primary, and
 300 secondary evaluation factor layers). Decision layer A is the site selection of landfill, primary layer
 301 B contains five criteria, secondary layer C includes 20 sub-criteria.

302 Ten experts were invited to fill out questionnaires to score the criteria. Among
 303 them were five professors who have been engaged in solid waste research for more than
 304 ten years, and five experts involved in urban planning. To improve the accuracy and

305 rationality of the evaluation, a numerical scale of 1-9 (**Table 1**) was employed to
 306 quantify the evaluation criteria of the constraint factor layer, which were used to
 307 construct pairwise comparison judgment matrices, respectively.

$$\begin{array}{c|cccc}
 A & B_1 & B_2 & \cdots & B_n \\
 B_1 & a_{11} & a_{12} & \cdots & a_{1n} \\
 B_2 & a_{21} & a_{22} & \cdots & a_{2n} \\
 \vdots & \vdots & \vdots & \ddots & \vdots \\
 B_n & a_{n1} & a_{n2} & \cdots & a_{nn}
 \end{array}$$

309 **Table 1**

310 Relative importance scale.

Scaling a_{ij}	1	3	5	7	9
The degree to which the i factor is stronger than the j factor	Equal	Slightly stronger	Strong	Very strong	Absolutely strong

311 Among these, 2, 4, 6, and 8 corresponded to the importance of 1, 3, 5, 7, and 9
 312 respectively.

313 The essence of calculating a relative weight is to calculate the normalized value
 314 \bar{W}_i and the maximum eigenvalue λ_{\max} of the eigenvector of the judgment matrix (Eq. 1-
 315 3) (Vaverkova et al., 2018).

$$W_i = n \sqrt[n]{\prod_{j=1}^n a_{ij}} \quad i = 1, 2, \dots, n \quad (1)$$

317
$$\bar{W}_i = \frac{W_i}{\sum_{i=1}^n W_i} \quad i = 1, 2, \dots, n \quad (2)$$

318
$$\lambda_{\max} = \sum_{i=1}^n \frac{(A\bar{W})_i}{n\bar{W}_i} \quad i = 1, 2, \dots, n \quad (3)$$

319 Where, W_i represents the eigenvector of the judgment matrix, \bar{W}_i represents the
 320 normalized value of the eigenvector and satisfies $0 < \bar{W}_i \leq 1$, λ_{\max} represents the
 321 maximum eigenvalue of the judgment matrix, and n represents the number of criteria.

322 Calculation for the consistency metric CI (Eq. 4):

323
$$CI = \frac{\lambda_{\max} - n}{n - 1} \quad (4)$$

324 When $\lambda_{\max} = n$, $CI = 0$ means that the matrix is completely consistent. When $\lambda_{\max} \neq n$,
 325 and the average random consistency metric RI (**Table 2**) is introduced to determine the
 326 size of CI . The higher the value of CI , the greater the probability of random deviation
 327 from consistency.

328 **Table 2**

329 Mean random consistency index.

Matrix order	3	4	5	6	7	8	9	10	11	12	13
RI	0.58	0.90	1.12	1.24	1.32	1.41	1.45	1.49	1.51	1.54	1.56

330 Calculation for the consistency ratio CR (Eq. 5):

331
$$CR = \frac{CI}{RI} \tag{5}$$

332 When $CR < 0.1$, it denotes that the degree of inconsistency of the judgment matrix is
 333 within the controllable range, and its normalized eigenvector can be used as the weight
 334 vector through the consistency test; if $CR > 0.1$, it means that the consistency of the
 335 judgment matrix deviates too much, the judgment matrix should be adjusted.

336 We employed MATLAB software to calculate the relative weight, maximum
 337 eigenvalue, consistency index and consistency ratio of each evaluation criterion, where
 338 after the criterion weight was obtained (**Table 3**). Further details are presented in **Tables**
 339 **D1 through D6** in Appendix D.

340 **Table 3**

341 Evaluation Criterion Weight.

Criteria B	Relative weight W_{B_i}	Sub-criteria C	Relative weight W_{C_i}	Normalized weight \bar{W}_{C_i}
Hydrogeologica 1 B ₁	0.3192	Groundwater depth C ₁	0.3984	0.1272
		Groundwater quality C ₂	0.1072	0.0342
		Groundwater richness C ₃	0.2443	0.0780
		Distance from faults C ₄	0.1392	0.0444

		Distance from earthquake points C ₅	0.1109	0.0354
		Elevation C ₆	0.1769	0.0325
		Slope C ₇	0.4543	0.0836
Morphological	0.1840	Landform type C ₈	0.0960	0.0177
B ₂		NDVI C ₉	0.0960	0.0177
		Soil type C ₁₀	0.1769	0.0325
		Distance from surface water C ₁₁	0.3509	0.1120
Environmental	0.3192	Land use type C ₁₂	0.1890	0.0603
B ₃		Distance from settlements C ₁₃	0.3509	0.1120
		Distance from roads C ₁₄	0.1091	0.0348
		Precipitation C ₁₅	0.6667	0.0455
Climatic B ₄	0.0683	Temperature C ₁₆	0.3333	0.0228
		Distance from ecological function reserves C ₁₇	0.4554	0.0498
Socio-economic	0.1094	Population density C ₁₈	0.1409	0.0154
B ₅				

342 Mapping and analysis of criteria attributes based on fuzzy logic, S-shape,
343 triangular shape, and Gamma shape are commonly employed fuzzy membership
344 functions to determine fuzzy information in fuzzy logic (as shown in **Table 4**) (Barakat
345 et al., 2017). The effects of the 7 scenarios applied were investigated, aiming to obtain
346 the most suitable scenario to improve the accuracy of the results and optimize the
347 uncertainty of the evaluation criteria.

348 Scenario 1: All criteria employ the nonlinear fuzzy membership function (S shape)
349 to calculate the fuzzy membership.

350 Scenario 2: All criteria employ the linear fuzzy membership function (Triangular
351 shape) to calculate the fuzzy membership.

352 Scenario 3: All criteria employ the linear fuzzy membership function (Gamma
353 shape) to calculate the fuzzy membership.

354 Scenario 4: Criteria employ S and Triangular shapes to calculate the fuzzy
355 membership.

356 Scenario 5: Criteria employ S and Gamma shapes to calculate the fuzzy
357 membership.

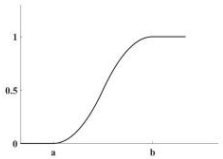
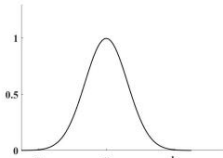
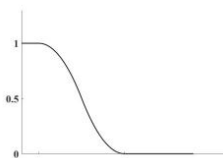
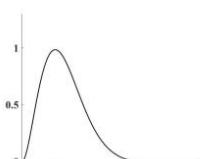
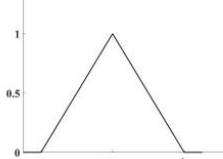
358 Scenario 6: Criteria employ Triangular and Gamma shapes to calculate the fuzzy
359 membership.

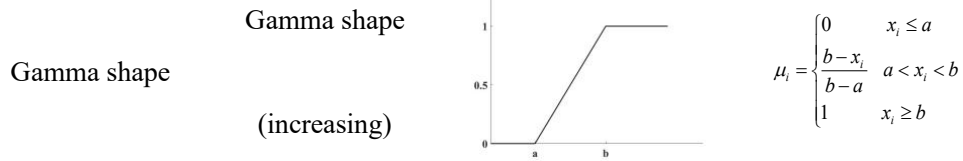
360 Scenario 7: Criteria employ S, Triangular, and Gamma shapes to calculate the fuzzy

361 membership.

362 **Table 4**

363 Fuzzy membership function.

Fuzzy Membership Function		Figure	Formula
S-shape	S-shape (increasing)		$\mu_i = \begin{cases} 0 & x_i \leq a \\ 2\left(\frac{x_i - a}{b - a}\right)^2 & a < x_i < b \\ 1 & x_i \geq b \end{cases}$
	S-Shape (general)		$\mu_i = \begin{cases} 0 & x_i \leq a \\ 2\left(\frac{x_i - a}{m - a}\right)^2 & a < x_i \leq m \\ 2\left(\frac{x_i - b}{b - m}\right)^2 & m < x_i < b \\ 0 & x_i \geq b \end{cases}$
	S-shape (decreasing)		$\mu_i = \begin{cases} 1 & x_i \leq a \\ 2\left(\frac{x_i - b}{b - a}\right)^2 & a < x_i < b \\ 0 & x_i \geq b \end{cases}$
	S-shape (individual)		$\mu_i = \begin{cases} 2\left(\frac{x_i - a}{a}\right)^2 & x_i \leq a \\ 2\left(\frac{x_i - b}{b - a}\right)^2 & a < x_i < b \\ 0 & x_i \geq b \end{cases}$
Triangular shape	Triangular shape (general)		$\mu_i = \begin{cases} 0 & x_i \leq a \\ \frac{x_i - a}{m - a} & a < x_i \leq m \\ \frac{b - x_i}{b - m} & m < x_i < b \\ 0 & x_i \geq b \end{cases}$



364 In **Table 4**, x_i denotes the attribute feature value of the i evaluation sub-criteria, μ_i
 365 represents the degree of membership, and a, b represents the interval value of the i
 366 evaluation criteria with different suitability grades, $m = \frac{a+b}{2}$.

367 For this study, we established an overlay model of multi-source layers by using
 368 the GIS spatial analysis tool. The weight of the evaluation criteria was multiplied by
 369 the fuzzy membership degree to obtain the Landfill Suitability Index (LSI) of the Hexi
 370 Corridor landfill site by a weighted average. The specific formula is as follows (Eq.
 371 (6)):

$$372 \quad LSI = \sum W_i \cdot \mu_i \quad (6)$$

373 Where, LSI denotes the suitability index, W_i denotes the comprehensive weight of the
 374 evaluation sub-criteria, and μ_i denotes the fuzzy membership degree of the evaluation
 375 criteria.

376 2.6. GIS spatial analysis

377 On the basis of a unified projected coordinate system, the application of GIS buffer
 378 analysis, network analysis, data reclassification, neighborhood analysis, overlay
 379 analysis, raster calculator, model builder, and other extended tools were used for data

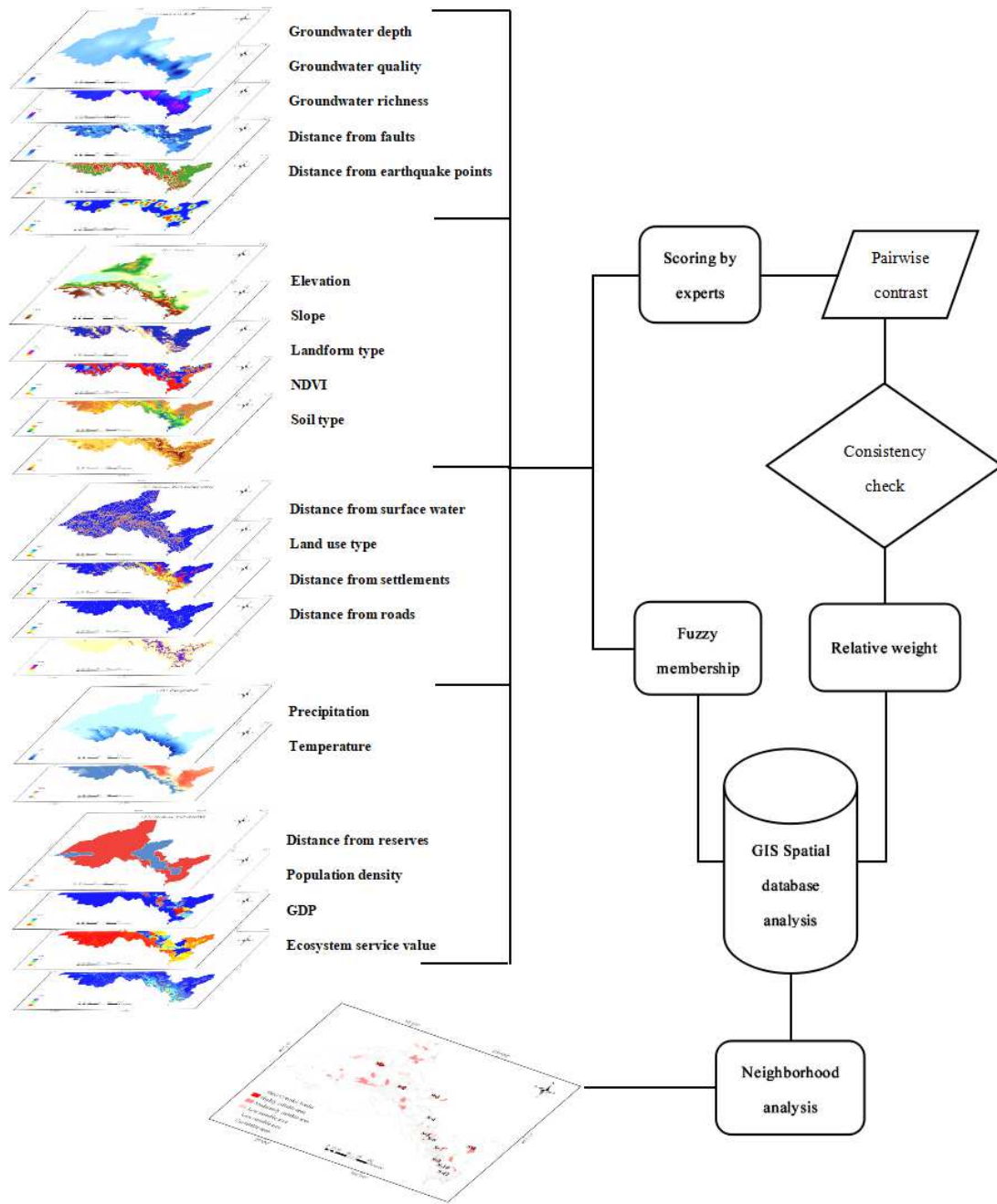
380 processing.

381 2.6.1. Buffer analysis

382 The primary purpose of buffer analysis is to restrict the range of vector data through
383 the establishing of a special distance radius or boundary. Vector data is segmented by
384 point, polyline, and polygon elements (Khan et al., 2018). According to the
385 requirements of urban construction planning, the specified range is utilized as the radius
386 of influence to establish buffer zones for faults, earthquake points, surface water,
387 settlements, roads, and ecological function reserves, such that the suitable construction
388 area is within a reasonable distribution range.

389 2.6.2. Model builder modeling overlay

390 Initially, we utilized the raster calculator input function and map algebra grammar
391 in ArcGIS to calculate the evaluation criteria and obtain the attribute grading results.
392 Secondly, the optimal weight was obtained by expert scoring, and the fuzzy evaluation
393 matrix was determined by the membership degree. Finally, the Model builder tool was
394 employed to model according to the *LSI*, superposition the attribute grading results of
395 the evaluation criterion, determine the optimal weight and the fuzzy evaluation matrix,
396 and obtain the LSSR (**Fig. 4**). According to the CNS, classified areas smaller than the
397 waste disposal area were unsuitable. Therefore, once the LSSR are smoothed, area
398 screening was required to eliminate areas that did not meet the requirements to ensure
399 the accuracy and rationality of the results.



400

401 **Fig. 4.** Flow chart of LSS modeling, which includes 20 normalized layers of criteria. GIS spatial

402 analysis was used to calculate its weight and fuzzy membership degree, and obtain the LSSR.

403 2.7. Group fuzzy MULTIMOORA

404 MULTIMOORA presents a robust result by combining the subordination rank

405 based on the dominance theory. There are three methods for MULTIMOORA: Ratio

406 System, Reference Point Approach, and Full Multiplicative Form. In addition,
 407 MULTIMOORA could be beneficial in a general form of a decision-making problem
 408 in which “positive “and “negative” sub-criteria exist besides noting to a “robust” final
 409 outcome (Hafezalkotob et al., 2019). In this study, the fuzzy group extension of
 410 MULTIMOORA is employed, which has the following steps:

411 Fuzzy ratio system:

412 Step 1 A fuzzy decision matrix is constructed, $x_{ij}^{[k]} = (x_{ij1}^{[k]}, x_{ij2}^{[k]}, x_{ij3}^{[k]})$ represent
 413 the response of expert k to sub-criteria j in place of alternative i . The decision matrix
 414 should be aggregated as follows.

$$415 \quad x_{ij} = \left(\frac{1}{h} \sum_{k=1}^h x_{ij1}^{[k]}, \frac{1}{h} \sum_{k=1}^h x_{ij2}^{[k]}, \frac{1}{h} \sum_{k=1}^h x_{ij3}^{[k]} \right) \quad (7)$$

416 Step 2 The decision matrix is normalized based on the following vector method,

417 where m is the number of alternatives.

$$418 \quad x_{ij}^* = \left(\frac{x_{ij1}}{\sqrt{\sum_{i=1}^m x_{ij1}^2}}, \frac{x_{ij2}}{\sqrt{\sum_{i=1}^m x_{ij2}^2}}, \frac{x_{ij3}}{\sqrt{\sum_{i=1}^m x_{ij3}^2}} \right) \quad (8)$$

419 Step 3 The weighted normalized decision matrix was used to calculate the relative
 420 importance of the alternatives (Eq.8). where g is the number of positive criteria, n is the
 421 number of criteria, and w is the weight of the sub-criteria j .

$$422 \quad y_i = \left(\sum_{j=1}^g (w_j \otimes x_{ij}^*) \right) - \left(\sum_{j=g+1}^n (w_j \otimes x_{ij}^*) \right) \quad (9)$$

423 Step 4 The best alternative and the ranking of this method is obtained as follows.

$$424 \quad Z_{F_RS} = \left\{ Z_i \mid \max_i y_i \right\} \quad (10)$$

425 Fuzzy reference point approach:

426 Step 1 and Step 2 are the same as Fuzzy ratio system, and the vector of reference

427 point is calculated as follows.

$$428 \quad x_j = \begin{cases} \left(\max_i x_{ij1}^*, \max_i x_{ij2}^*, \max_i x_{ij3}^* \right), & \text{for positive criteria} \\ \left(\min_i x_{ij1}^*, \min_i x_{ij2}^*, \min_i x_{ij3}^* \right), & \text{for negative criteria} \end{cases} \quad (11)$$

429 Step 3 The weighted normalized decision matrix was used to calculate the relative

430 importance of the alternatives (Eq.11), where w is the weight of the sub-criteria j .

$$431 \quad y_i = \max_j d \left[(w_j \otimes x_i), (w_j \otimes x_j^*) \right] \quad (12)$$

432 Step 4 The best alternative and the ranking of this method is obtained as follows.

$$433 \quad Z_{F_RP} = \left\{ Z_i \mid \max_i y_i \right\} \quad (13)$$

434 Fuzzy full multiplicative form:

435 Step 1 and Step 2 are the same as Fuzzy ratio system.

436 Step 3 The weighted normalized decision matrix was used to calculate the relative

437 importance of the alternatives (Eq.13). where g is the number of positive criteria, n is

438 the number of criteria, and w is the weight of the sub-criteria j .

$$439 \quad y_i = \frac{\prod_{j=1}^g (x_{ij}^*)^{w_j}}{\prod_{j=g+1}^n (x_{ij}^*)^{w_j}} \quad (14)$$

440 Step 4 The best alternative and the ranking of this method is obtained as follows.

$$441 \quad Z_{F_MF} = \left\{ Z_i \mid \max_i y_i \right\} \quad (15)$$

442 **3. Results and discussion**

443 Based on the FAHP-GIS model, the LSS of MSW in the ecologically fragile area of
444 the Hexi Corridor was studied for the first time. According to expert judgment in the
445 criteria, hydrogeological and environmental factors were the most important criteria for
446 landfills, with the weights of both being 0.3192. The climatic weight was 0.0683, which
447 had a relatively low impact on the LSSR. In the sub-criteria, the groundwater depth had
448 the greatest impact on site selection, with a weight of 0.1272.

449 According to the *LSI*, we selected suitable areas for landfills in the Hexi Corridor
450 (**Fig. 5**). The range of *LSI* was between 0 and 1, whereas the attribute value was
451 divided by three grades: "suitable area (1-0.8), less suitable area (0.8-0.6), unsuitable
452 area (0.6-0)".

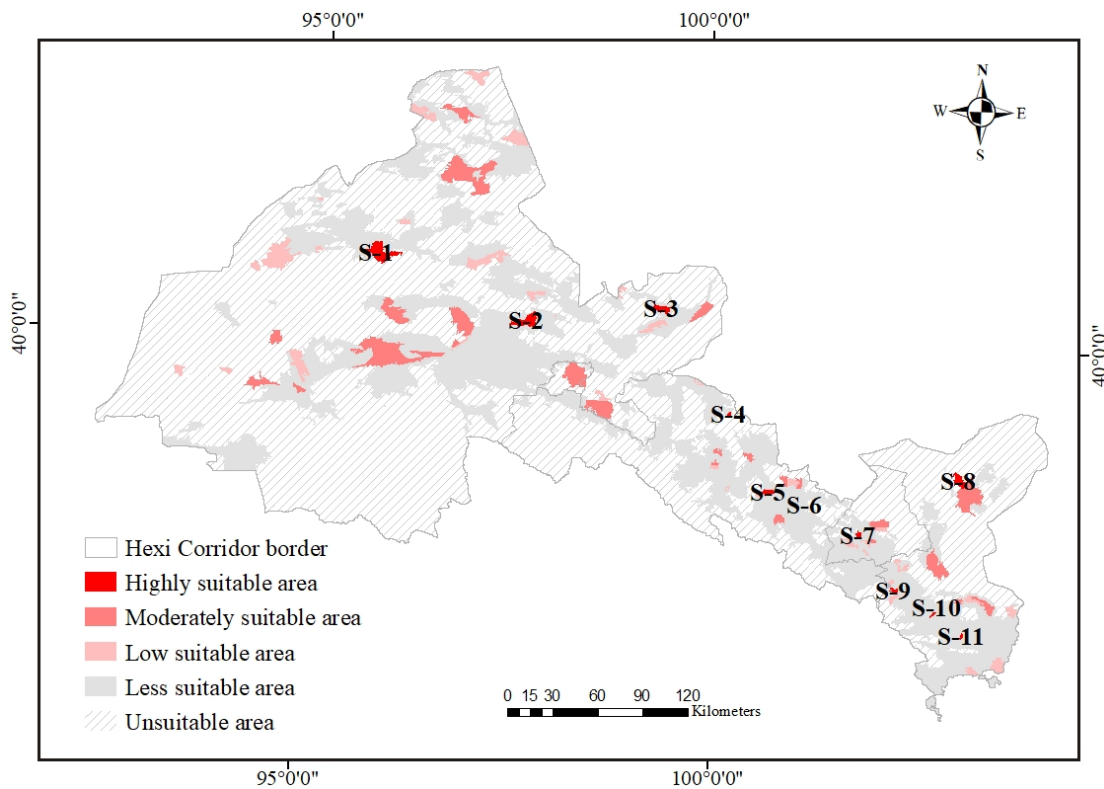
453 The comparison of the scenarios' application results with the initial results
454 revealed a slight degree of variation. The most suitable area ratios for scenarios 1-7
455 were 0.06, 0.07, 0.07, 0.05, 0.05, 0.06, 0.03. Furthermore, the Spearman's correlation
456 coefficient values of scenario 1, compared with those of other scenarios, confirmed the
457 similarities. As the results observed suggest, scenario 2, 3 accounted for the highest
458 degree of variation in area ratios, as it reduced Spearman's correlation coefficient value
459 (0.94), the coefficient scores of scenarios 4-7 were all 1. The result demonstrated that

460 setting the corresponding membership function to reflect its logical relationship and
461 ambiguity according to the different standard attributes can improve the reliability of
462 the results.

463 We compared the existing location coordinates of 28 landfill sites that conformed
464 to the CNS and the LSSR of Scenario 7. The results revealed that 26 sites were located
465 in suitable areas, one site was located in a less suitable area, and one site was located in
466 an unsuitable area, with an accuracy of 93%. This illustrated the scientific reliability of
467 the LSSR based on the integrated FAHP-GIS model. Suitable areas were characterized
468 as having low groundwater depth, flat terrain, mostly bare land, a 300 m distance from
469 roads, and at least a 2000 m distance from settlements with low land use value. The less
470 suitable areas were characterized by a lack of surface water development, moderate
471 elevation, within 500 m of the traffic line, and distance from settlements of 2000m. The
472 unsuitable areas were characterized by complex terrain, large topographic relief, large
473 soil sediment concentrations, with the distance from surface water of from 50 m to 500
474 m, and distance from settlements of less than 1000 m, with high land use value.

475 Encompassing the study region as a whole, the unsuitable areas accounted for the
476 largest proportion (0.67) with an area of $1.80 \times 10^5 \text{ km}^2$, which was mainly distributed
477 along the river. The less suitable areas accounted for a relatively large number (0.30),
478 with an area of $8.20 \times 10^4 \text{ km}^2$, which was primarily distributed in the central part of the
479 study area. The suitable area occupied a small area (0.03), with an area of $0.8 \times 10^4 \text{ km}^2$,
480 scattered across various cities. At the municipal scale (**Fig. E1**, Appendix E), the

481 unsuitable areas were evenly distributed in each city. Jiuquan accounted for the largest
 482 proportion of 0.7, with an area of $1.34 \times 10^5 \text{ km}^2$, whereas Zhangye had the lowest
 483 proportion. The less suitable areas were mainly distributed in Zhangye with a
 484 proportion of 0.46, having an area of $1.88 \times 10^4 \text{ km}^2$, with the lowest proportion in
 485 Jiuquan. The suitable areas were primarily distributed in Jiuquan with a proportion of
 486 0.05, covering an area of $9.60 \times 10^4 \text{ km}^2$, where Zhangye and Jinchang had the lowest
 487 proportion.



488
 489 **Fig. 5.** Site selection of MSW landfills in Hexi Corridor. The LSSR are graded according to color
 490 brightness. Brighter reds indicate better suitability, gray indicates less suitability, and the line fill
 491 indicates the unsuitable. A total of 11 candidate sites were selected in the Hexi Corridor.

492 The landfill suitability values of the study area were divided into three categories:

493 highly (1-0.934), moderately (0.934-0.867), and low suitable (0.867-0.800) by
494 employing the equal interval classification method. The results revealed that in the
495 suitable area ($8.0 \times 10^3 \text{ km}^2$), the area of highly suitable was $2.0 \times 10^2 \text{ km}^2$ (0.03), the area
496 of moderately suitable was $4.4 \times 10^3 \text{ km}^2$ (0.55), and the area of low suitable was
497 $3.4 \times 10^3 \text{ km}^2$ (0.42). We selected 11 candidate landfill sites and location coordinates that
498 conformed to the CNS for the Hexi Corridor. The daily MSW capacity of the candidate
499 sites was calculated according to the “Construction Standard of MSW Landfill Disposal
500 Engineering Project” (**Table F1 and F2**, Appendix F).

501 There were three candidate landfills (S-1, S-2 and S-3) in Jiuquan. Among these, S-
502 1 and S-2 had a capacity of more than 1200 tons/day of MSW, while S-3 could hold
503 500 to 1200 tons/Day of MSW. Jiayuguan had no optimal site. There were three
504 candidate landfill sites in Zhangye (S-4, S-5 and S-6), among which S-4 and S-6 had
505 the capacity to contain MSW at less than 200 tons/day, whereas S-5 could contain 500
506 to 1200 tons/day of MSW. There was one most suitable site (S-7) in Jinchang that could
507 be used as a candidate landfill, with a capacity of 200 to 500 tons/day of MSW. There
508 was a total of four candidate landfills in Wuwei (S-8, S-9, S-10, and S-11). Among these,
509 S-8 had the capacity to accommodate more than 1200 tons/day of MSW, whereas S-9
510 could absorb 500 to 1200 tons/day of MSW, S-10 could hold less than 200 tons/day of
511 MSW, and S-11 could accommodate 200 to 500 tons/day of MSW (**Table F2**, Appendix
512 F). The rankings for the fuzzy ratio system, fuzzy reference point approach, and fuzzy
513 full multiplicative form are obtained based on Eq. 9, 12, and 14, respectively. The three

514 subordinate rankings are integrated exploiting the dominance theory. The outcomes of
515 the three approaches and the final ranking are listed in **Table G1** in Appendix G. Based
516 on the three approaches of the group fuzzy MULTIMOORA, the suitable site is S-2.
517 Hence, since the outcomes are consistent, it can be decided that in the face of
518 inconsistent criteria, the methodology used was suitable and robust and the resultant
519 findings of the research logical and accurate.

520 **4. Conclusion**

521 For this study, we initially developed the proper criteria for evaluating the suitability
522 of the LSSR in the Hexi Corridor. The main conclusions were as follows:

523 The uncertainty of AHP expert scoring was reduced and the decision efficiency of
524 spatial analysis was improved. The synthesis of 20 multi-source data and multiple fuzzy
525 membership functions proved a new model for the rational planning of MSW landfill
526 sites in arid areas with fragile ecological environments, to realize LSSR within the Hexi
527 Corridor. To reduce the uncertainty of AHP, proper membership functions were selected
528 for each evaluation criterion, including the S-shape (increasing), (decreasing), (general),
529 (individual), Triangular shape (general), and Gamma shape (increasing). From the
530 analysis of the results, it was shown that the spatial distribution characteristics differed
531 greatly as to the suitability of Hexi Corridor landfills.

532 The verification results based on field investigations revealed that this strategy was
533 feasible and highly accurate. Specifically, among 28 landfills, 26 were located in

534 suitable areas, with an accuracy of 93%. There were two possible reasons why two
535 landfills did not conform to the verification results. Urban growth leads to changes in
536 regional population density, economy, and land use. The ecological environment is
537 extremely fragile in the study area, and the ecological function reserve was expanded.

538 A number of ideal MSW landfill sites were located, with 11 landfill site candidates
539 in total selected, according to the CNS. Among them, three candidates were located in
540 Jiuquan and Zhangye, one candidate in Jinchang, and four candidates in Wuwei. The
541 group fuzzy MULTIMOORA method was applied because of its high practicality in
542 solving decision making problems to reach the optimal alternative. Consequently,
543 Group fuzzy MULTIMOORA can effectively result in a reliable ranking of the
544 candidate landfill sites. From an economic perspective, the accessibility of landfills
545 based on spatial clustering could reduce transportation costs, while providing a
546 scientific basis for optimizing the transport of waste.

547 This research method might also be employed to address MSW disposal problems
548 in other similar areas, while providing decision support for waste disposal and
549 environmental protection. This study incorporated three innovations for the LSS
550 process. Initially, 20 multi-source data items were collected and multiple fuzzy
551 membership functions were introduced to reduce the uncertainty of expert scoring.
552 Secondly, the Hexi Corridor, which is extremely vulnerable to ecological fragility, was
553 selected for case studies. A total of 11 candidate landfill sites were identified that
554 conformed to the CNS, which demonstrated that this method was applicable in arid

555 areas. Finally, the LSSR were compared with existing landfill sites in accordance with
556 the CNS, and the accuracy was higher. Consequently, we illustrated the appropriateness
557 and reliability of this novel siting mode, which evaluated the suitability of landfill sites
558 from the perspective of environmental health risks, while providing scientific
559 references for decision-makers to support urban planning and environmental protection.

560

561 **Appendix Supplementary data**

562

563 **Appendix A**

564

565

566 **Table A1**

567 Data Format and Source.

Dataset	Format	Data Source
Groundwater depth、	Vector (Point)	Gansu Groundwater Report (Gansu Water Resources
Groundwater quality		Department) (http://slt.gansu.gov.cn/)

		" Gansu Hydrogeological Map "
Groundwater richness	Vector (Polygon)	(Gansu Bureau of Geology and Mineral Hydrogeology engineering Geological Exploration Institute) (http://www.gssgy.com/)
		" Gansu Hydrogeological Map "
Faults	Vector (Polyline)	(Gansu Bureau of Geology and Mineral Hydrogeology engineering Geological Exploration Institute) (http://www.gssgy.com/)
		"China Historical Earthquake Catalog"
Earthquake points	Vector (Point)	(Gansu Earthquake Agency) (http://www.gsdzj.gov.cn/)
30m SRTM Elevation	Raster	USGS Earth Explorer (https://earthexplorer.usgs.gov/)
		"Landscape Atlas of the People's Republic of China (1: 1 million)"
Landform type	Raster	Resource and Environmental Science and Data Center, Chinese Academy of Sciences (http://www.resdc.cn/)
NDVI	Raster	MODIS (https://modis.gsfc.nasa.gov/)

		"The Soil Atlas of the People's Republic of China (1: 1 million)"
Soil type	Raster	Resource and Environmental Science and Data Center, Chinese Academy of Sciences (http://www.resdc.cn/)
surface water	Vector (Polyline)	National Catalogue Service for Geographic Information (https://webmap.cn/)
30m Land use type	Raster	Resource and Environmental Science and Data Center, Chinese Academy of Sciences(http://www.resdc.cn/)
Settlements	Vector (Point)	National Catalogue Service for Geographic Information (https://webmap.cn/)
Roads	Vector (Polygon)	National Catalogue Service for Geographic Information (https://webmap.cn/)
Precipitation	Raster	Resource and Environmental Science and Data Center, Chinese Academy of Sciences (http://www.resdc.cn/)
Temperature	Raster	Resource and Environmental Science and Data Center, Chinese Academy of Sciences (http://www.resdc.cn/)
Ecological function reserves	Vector (Polygon)	Portal website of Gansu Forestry and Grass Bureau and its administrative departments(http://lycy.gansu.gov.cn/)

Population density	Raster	Resource and Environmental Science and Data Center, Chinese Academy of Sciences(http://www.resdc.cn/)
GDP	Raster	Resource and Environmental Science and Data Center, Chinese Academy of Sciences(http://www.resdc.cn/)
Ecosystem service value	Raster	Resource and Environmental Science and Data Center, Chinese Academy of Sciences(http://www.resdc.cn/)

568 **Appendix B**

569

570

571 **Table B1**

572 Suitability grade of evaluation criterion and Fuzzy membership function.

Criteria B	Sub-criteria C	Unsuitable	Less suitable	Suitable	Fuzzy
					membership function
Hydrogeological B ₁	Groundwater depth C ₁ (m)	<15	15-30	>30	S-Function (increasing)
	Groundwater quality C ₂	V	III、IV	I、II	S-Function (decreasing)

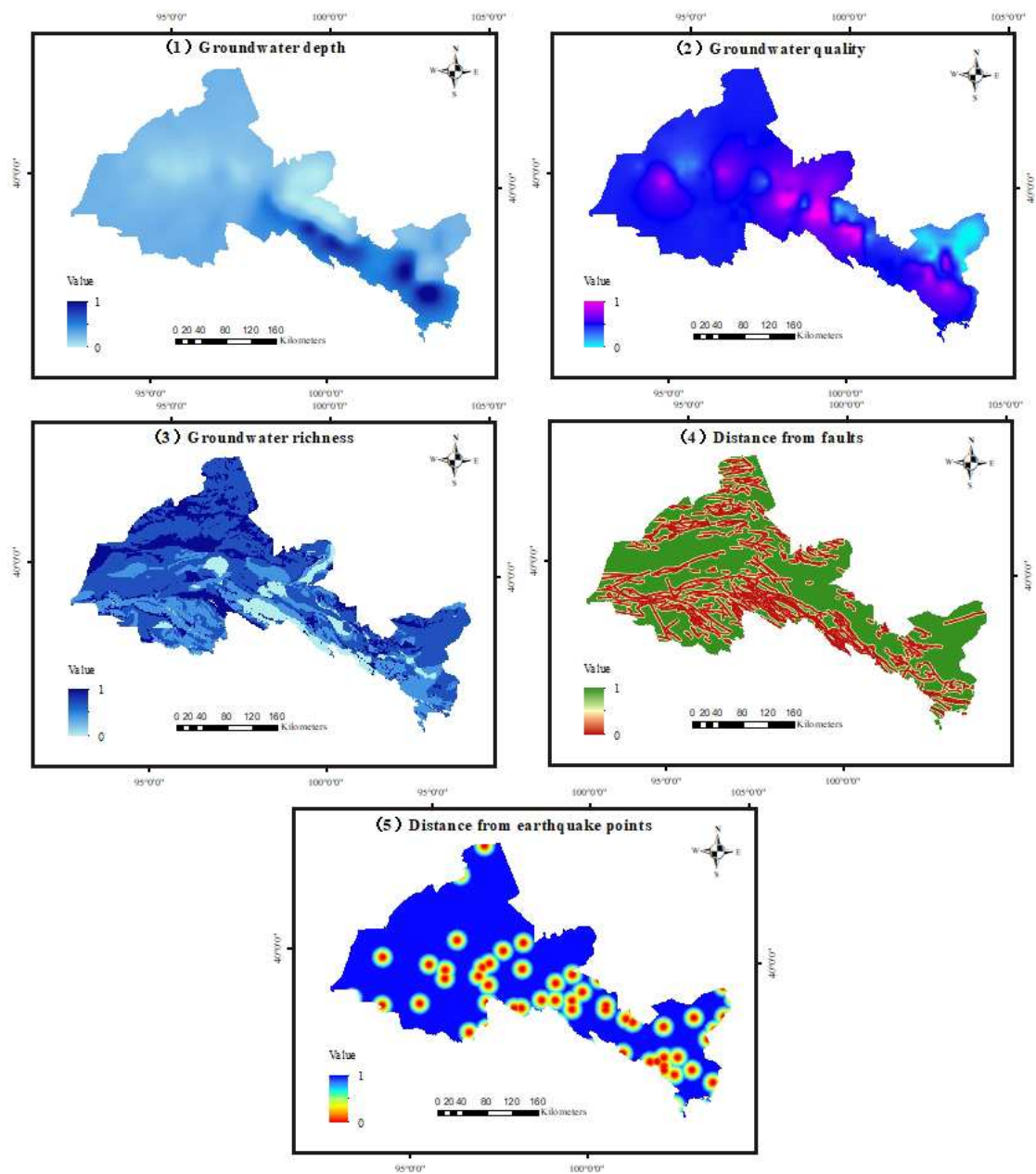
Morphological B ₂	Groundwater richness C ₃ (m ³ /L)	>1000	100-1000	<100	S-Function (decreasing)
	Distance from faults C ₄ (m)	<1000	1000-6000	>6000	Gamma Function (increasing)
	Distance from earthquake points C ₅ (m)	<500	500-5000	>5000	Gamma Function (increasing)
	Elevation C ₆ (m)	>2200	1500-2200	<1500	S-Function (decreasing)
	Slope C ₇	>20%	5%-20%	8%	S-Function (individual)c
	Landform type C ₈	Mountains	Terraces, hills	Plains	S-Function (decreasing)
	NDVI C ₉	>0.8	0.2-0.8	<0.2	S-Function (decreasing)
	Soil type C ₁₀	Aquatic soil, leached soil,	Alpine soil, desert soil,	Saline soil	S-Function

		anthropogen	semi-aqueous		(decreasing)
		ic soil	soil, rock		
			soil,		
			calcareous		
			soil, arid soil,		
			primordial		
			soil, semi-		
			leached soil		
	Distance from				Gamma
	surface water C ₁₁	<150	150-1000	>1000	Function
	(m)				(increasing)
		Water,			
		snow,	Grassland,		S-Function
Environmental B ₃	Land use type C ₁₂	farmland,	shrubland,	bare land	(decreasing)
		woodland	wetland		
	Distance from				Gamma
	settlements C ₁₃	<800	800-3000	>3000	Function
	(m)				(increasing)
	Distance from roads	<500 >1	500-1500	1000	S-Function

	C ₁₄ (m)	500			(general)
Climatic B ₄	Precipitation C ₁₅ (mm)	>300	180-300	<180	S-Function (decreasing)
	Temperature C ₁₆ (°C)	<2 >10	2-10		Triangular Function (general)
Socio-economic B ₅	Distance from ecological function reserves C ₁₇ (m)	<3000	3000-9000	>9000	Gamma Function (increasing)
	Population density C ₁₈	>200	50-200	<100	S-Function (decreasing)
	GDP C ₁₉	<200 >100 0	200-1000	600	S-Function (general)
	Ecosystem service value C ₂₀	>15000	5000-15000	<5000m	S-Function (decreasing)

573 **Appendix C**

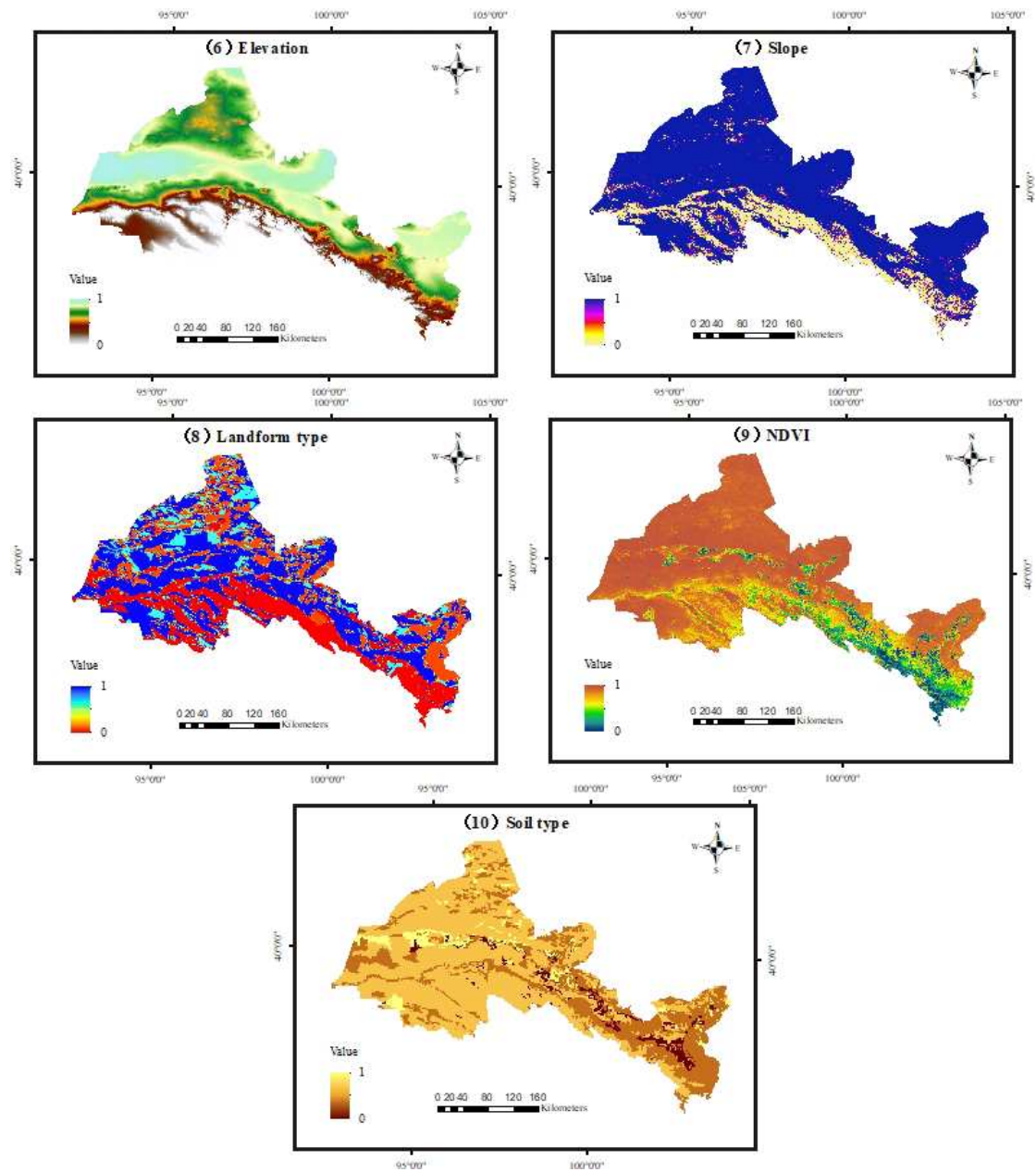
574



576

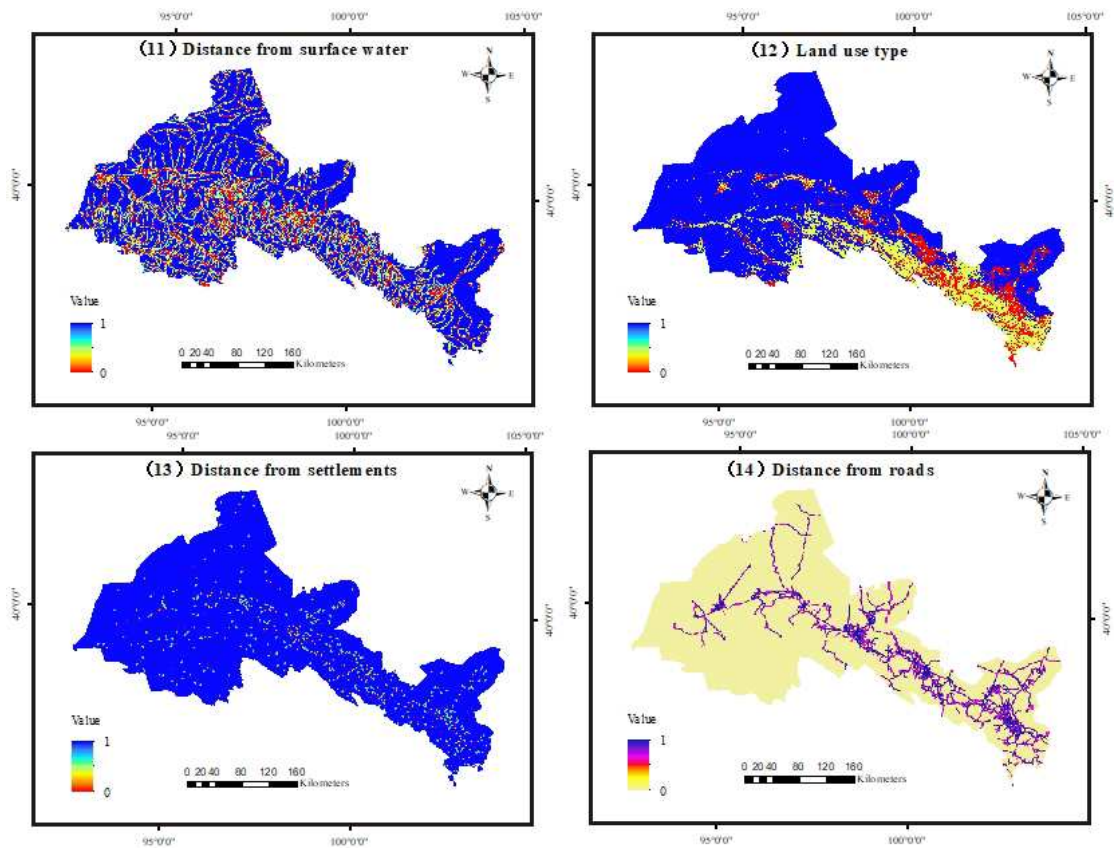
577 **Fig. C1.** Hydrogeological factors. (1) groundwater depth, (2) groundwater quality, (3) groundwater

578 richness, (4) distance from faults, (5) distance from earthquake points.



579

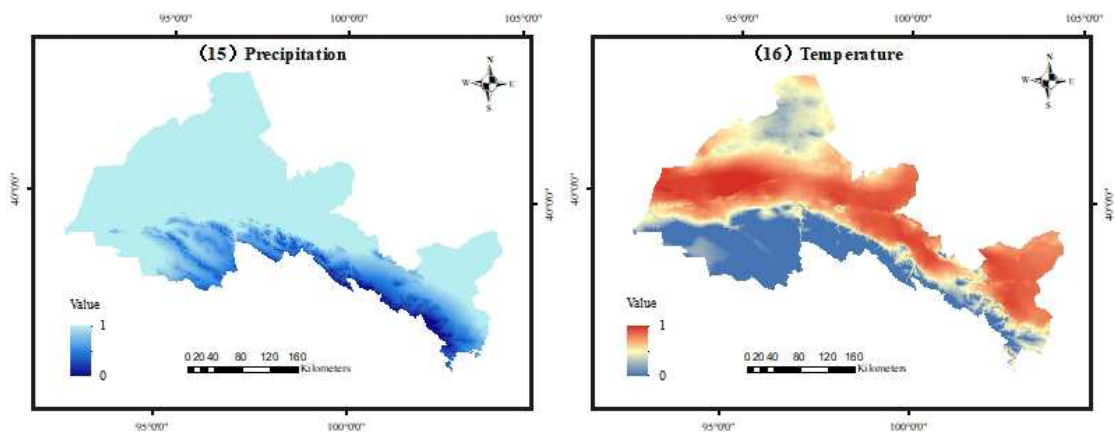
580 **Fig. C2.** Morphological factors. (6) elevation, (7) slope, (8) landform type, (9) NDVI, (10) soil type.



581

582 **Fig. C3.** Environmental factors. (11) distance from surface water, (12) land use type, (13) distance

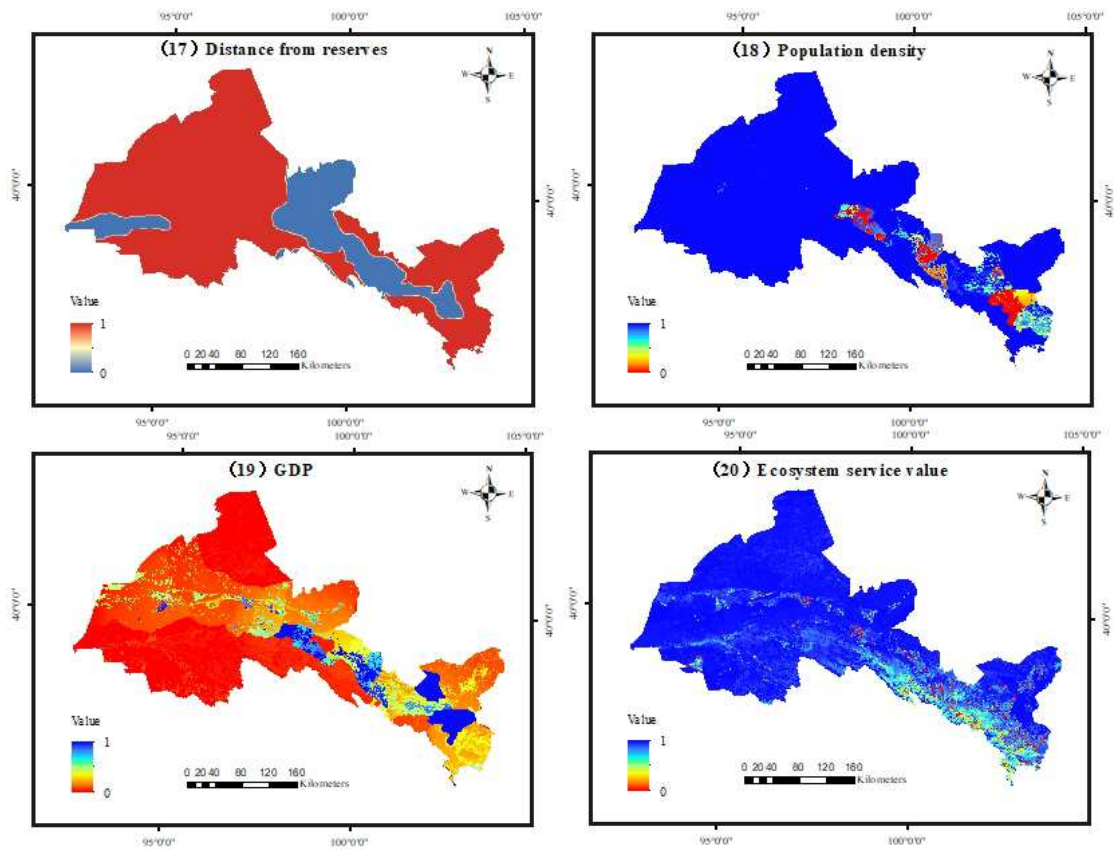
583 from settlements, (14) distance from roads.



584

585 **Fig. C4.** Climatic factors. (15) precipitation, (16) temperature.

586



587

588 **Fig. C5.** Socio-economic factors. (17) distance from ecological function reserves, (18) population
 589 density, (19) GDP, (20) ecosystem service value.

590 **Appendix D**

591

592

593 **Table D1**

594 Judgment matrix table of objective A and Criteria B₁₋₅.

Site	Hydrogeolog	Morphologic	Environment	Socio-	Relative
selection of	ical B ₁	al B ₂	al B ₃	economic B ₅	weight W_{B_i}
			Climatic B ₄		

landfill A						
Hydrogeological B ₁	1	2	1	4	3	0.3192
Morphological B ₂	1/2	1	1/2	3	2	0.1840
Environmental B ₃	1	2	1	4	3	0.3192
Climatic B ₄	1/4	1/3	1/4	1	1/2	0.0683
Socio-economic B ₅	1/3	1/2	1/3	2	1	0.1094

$$\lambda_{\max} = 5.0364, CI=0.0091, RI=1.12, CR=0.0081$$

595 **Table D2**

596 Criterion B₁ and Criteria C₁₋₅ Judgment Matrix.

Hydrogeological B ₁	Groundwater depth C ₁	Groundwater quality C ₂	Groundwater richness C ₃	Distance from faults C ₄	Distance from earthquake	Relative weight W_{C_i}	Normalized weight \bar{W}_{C_i}
--------------------------------	-------------------------------------	---------------------------------------	--	--	--------------------------	------------------------------	--------------------------------------

points C ₅							
Groundwater depth C ₁	1	3	2	3	4	0.3984	0.1272
Groundwater quality C ₂	1/3	1	1/2	1	1/2	0.1072	0.0342
Groundwater richness C ₃	1/2	2	1	2	3	0.2443	0.0780
Distance from faults C ₄	1/3	1	1/2	1	2	0.1392	0.0444
Distance from earthquake points C ₅	1/4	2	1/3	1/2	1	0.1109	0.0354
$\lambda_{\max} = 5.1944, CI = 0.0486, RI = 1.12, CR = 0.0434$							

597 **Table D3**

598 Criterion B₂ and Criteria C₆₋₁₀ Judgment Matrix.

Morphological B ₂	Elevation C ₆	Slope C ₇	Landform type C ₈	NDVI C ₉	Soil type C ₁₀	Relative weight W_{C_i}	Normalized weight \bar{W}_{C_i}
Elevation C ₆	1	1/3	2	2	1	0.1769	0.0277
Slope C ₇	3	1	4	4	3	0.4543	0.0497
Landform type C ₈	1/2	1/4	1	1	1/2	0.0960	0.0851
NDVI C ₉	1/2	1/4	1	1	1/2	0.0960	0.0150
Soil type C ₁₀	1	1/3	2	2	1	0.1769	0.0851

$$\lambda_{\max} = 5.0264, CI=0.0066, RI=1.12, CR=0.0059$$

599 **Table D4**

600 Criterion B₃ and Criteria C₁₁₋₁₄ Judgment Matrix.

Environmental B ₃	Distance from surface water C ₁₁	Land use type C ₁₂	Distance from settlement C ₁₃	Distance from roads C ₁₄	Relative weight W_{C_i}	Normalized weight \bar{W}_{C_i}
Distance	1	2	1	3	0.3509	0.1120

from surface						
water C ₁₁						
Land use						
type C ₁₂	1/2	1	1/2	2	0.1890	0.0603
Distance						
from						
settlements	1	2	1	3	0.3509	0.1120
C ₁₃						
Distance						
from roads	1/3	1/2	1/3	1	0.1091	0.0348
C ₁₄						

$$\lambda_{\max} = 4.0104, CI=0.0035, RI=0.90, CR=0.0039$$

601 **Table D5**

602 Criterion B₄ and Criteria C₁₅₋₁₆ Judgment Matrix.

Climatic B ₄	Precipitation C ₁₅	Temperature C ₁₆	Relative weight W_{C_i}	Normalized weight \bar{W}_{C_i}
Precipitation C ₁₅	1	2	0.6667	0.0455
Temperature C ₁₆	1/2	1	0.3333	0.0228

$$\lambda_{\max} = 2, \text{ CI}=0, \text{ RI}=0, \text{ CR}=0$$

603 **Table D6**

604 Criterion B₅ and Criteria C₁₇₋₂₀ Judgment Matrix.

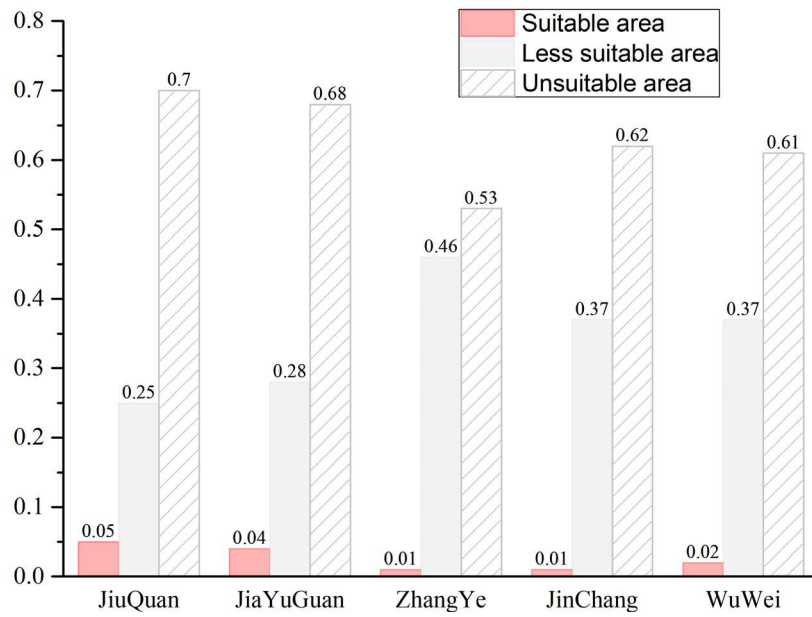
Socio-economic B ₅	Distance from ecological function reserves C ₁₇	Population density C ₁₈	GDP C ₁₉	Ecosystem service value C ₂₀	Relative weight W_{C_i}	Normalized weight \overline{W}_{C_i}
Distance from ecological function reserves C ₁₇	1	3	3	2	0.4554	0.0498
Population density C ₁₈	1/3	1	1	1/2	0.1409	0.0154
GDP C ₁₉	1/3	1	1	1/2	0.1409	0.0154
Ecosystem service value C ₂₀	1/2	2	2	1	0.2628	0.0287

$$\lambda_{\max} = 4.0104, \text{ CI}=0.0035, \text{ RI}=0.90, \text{ CR}=0.0039$$

605 **Appendix E**

606

607



608

609

Fig. E1. The proportion of suitability grade in Hexi Corridor.

610 **Appendix F**

611

612

613 **Table F1**

614 "Construction Standard of MSW Landfill Disposal Engineering Project". The landfill is divided into

615 four levels according to the area of the landfill. The smaller the area, the higher the level, and the

616 lower the amount of MSW to be disposed.

Landfill	I	II	III	IV
Area (Km ²)	>12	5-12	2-5	1-2
Amount of MSW (Tons/day)	>1200	500-1200	200-500	<200

617 **Table F2**

618 Candidate site latitude, longitude, area, and MSW disposal capacity. S-1 and S-2 had the highest
619 MSW disposal capacities, S-4, S-6, and S-10 had the lowest MSW disposal capacities.

City	Candidate site	Longitude	Latitude	Area	Amount of
				(Km ²)	MSW (Tons/day)
	S-1	95°46'40"E	40°56'28"N	41.83	>1200
JiuQuan	S-2	97°40'19"E	40°20'40"N	25.98	>1200
	S-3	99°22'45"E	40°29'38"N	10.67	500-1200
JiaYuGuan	-	-	-	-	-
	S-4	100°14'10"E	39°29'08"N	1.73	<200
ZhangYe	S-5	100°43'27"E	38°44'18"N	5.50	500-1200
	S-6	101°02'42"E	38°37'06"N	1.83	<200
JinChang	S-7	101°50'21"E	38°19'07"N	4.85	200-500

	S-8	103°05'06"E	38°19'30"N	15.00	>1200
	S-9	102°15'17"E	37°47'01"N	5.19	500-1200
WuWei	S-10	102°43'16"E	37°32'41"N	1.94	<200
	S-11	103°04'07"E	37°19'51"N	2.48	200-500

620 **Appendix G**

621

622

623 **Table G1**

624 Assessment values as well as subordinate and final rankings of alternative sites utilizing the Fuzzy
 625 MULTIMOORA method.

626

Altern atives	Fuzzy ratio system	Fuzzy referen ce point		Fuzzy full multiplicative form		Fuzzy MULTIMOOR A	
		y_i	Rank	y_i	Rank	y_i	Rank
S-1	(-0.128,-0.128,-0.125)	3	0.611	3	(6.233,6.195,6.158)	2	3
S-2	(-0.045,-0.043,-0.039)	1	0.339	1	(7.325,7.386,7.331)	1	1

S-3	(-0.174,-0.173,-0.171)	4	0.652	4	(5.391,5.474,5.252)	4	4
S-4	(-0.369,-0.364,-0.362)	10	0.797	10	(3.392,3.438,3.287)	10	10
S-5	(-0.221,-0.216,-0.214)	5	0.689	5	(4.990,4.925,4.871)	6	5
S-6	(-0.380,-0.375,-0.373)	11	0.822	11	(2.954,2.869,2.711)	11	11
S-7	(-0.299,-0.292,-0.292)	7	0.732	7	(4.771,4.857,5.040)	7	7
S-8	(-0.089,-0.083,-0.083)	2	0.558	2	(5.771,5.934,5.886)	3	2
S-9	(-0.266,-0.261,-0.259)	6	0.715	6	(5.174,5.378,5.221)	5	6
S-10	(-0.315,-0.311,-0.308)	8	0.769	9	(4.240,4.587,4.328)	8	8
S-11	(-0.341,-0.341,-0.339)	9	0.755	8	(3.870,3.929,3.965)	9	9

627

628

629 **References**

630 Afzali, A., Sabri, S., Rashid, M., Samani, J.M.V., Ludin, A.N.M., 2014. Inter-Municipal Landfill

631 Site Selection Using Analytic Network Process. *Water Resources Management* 28(8), 2179-2194.

632 <https://doi.org/10.1007/s11269-014-0605-3>.

633 Aksoy, E., San, B.T., 2016. USING MCDA AND GIS FOR LANDFILL SITE SELECTION:

634 CENTRAL DISTRICTS OF ANTALYA PROVINCE, in: Halounova, L., Li, S., Safar, V., Tomkova,

635 M., Rapant, P., Brazdil, K., Shi, W., Anton, F., Liu, Y., Stein, A., Cheng, T., Pettit, C., Li, Q.Q.,

636 Sester, M., Mostafavi, M.A., Madden, M., Tong, X., Brovelli, M.A., HaeKyong, K., Kawashima,

637 H., Coltekin, A. (Eds.), Xxiii Isprs Congress, Commission Ii. pp. 151-157.

638 Al-Ruzouq, R., Shanableh, A., Omar, M., Al-Khayyat, G., 2018. Macro and micro geo-spatial
639 environment consideration for landfill site selection in Sharjah, United Arab Emirates.
640 Environmental Monitoring And Assessment 190(3). <https://doi.org/10.1007/s10661-018-6538-1>.

641 Alavi, N., Goudarzi, G., Babaei, A.A., Jaafarzadeh, N., Hosseinzadeh, M., 2013. Municipal solid
642 waste landfill site selection with geographic information systems and analytical hierarchy process:
643 a case study in Mahshahr County, Iran. Waste Management & Research 31(1), 98-105.
644 <https://doi.org/10.1177/0734242x12456092>.

645 Aracil, C., Haro, P., Fuentes-Cano, D., Gomez-Barea, A., 2018. Implementation of waste-to-energy
646 options in landfill-dominated countries: Economic evaluation and GHG impact. Waste Management
647 76, 443-456. <https://doi.org/10.1016/j.wasman.2018.03.039>.

648 Asefi, H., Lim, S., 2017. A novel multi-dimensional modeling approach to integrated municipal
649 solid waste management. Journal Of Cleaner Production 166, 1131-1143.
650 <https://doi.org/10.1016/j.jclepro.2017.08.061>.

651 Asefi, H., Zhang, Y., Lim, S., Maghrebi, M., 2020. An integrated approach to suitability assessment
652 of municipal solid waste landfills in New South Wales, Australia. Australasian Journal Of
653 Environmental Management 27(1), 63-83. <https://doi.org/10.1080/14486563.2020.1719438>.

654 Bahrani, S., Ebadi, T., Ehsani, H., Yousefi, H., Maknoon, R., 2016. Modeling landfill site selection
655 by multi-criteria decision making and fuzzy functions in GIS, case study: Shabestar, Iran.
656 Environmental Earth Sciences 75(4). <https://doi.org/10.1007/s12665-015-5146-4>.

657 Barakat, A., Hilali, A., El Baghdadi, M., Touhami, F., 2017. Landfill site selection with GIS-based
658 multi-criteria evaluation technique. A case study in Beni Mellal-Khouribga Region, Morocco.
659 Environmental Earth Sciences 76(12). <https://doi.org/10.1007/s12665-017-6757-8>.

660 Beskese, A., Demir, H.H., Ozcan, H.K., Okten, H.E., 2015. Landfill site selection using fuzzy AHP
661 and fuzzy TOPSIS: a case study for Istanbul. Environmental Earth Sciences 73(7), 3513-3521.
662 <https://doi.org/10.1007/s12665-014-3635-5>.

663 Calabro, P.S., Gentili, E., Meoni, C., Orsi, S., Komilis, D., 2018. Effect of the recirculation of a
664 reverse osmosis concentrate on leachate generation: A case study in an Italian landfill. Waste
665 Management 76, 643-651. <https://doi.org/10.1016/j.wasman.2018.03.007>.

666 Davami, A.H., Moharamnejad, N., Monavari, S.M., Shariat, M., 2014. An Urban Solid Waste
667 Landfill Site Evaluation Process Incorporating GIS in Local Scale Environment: A Case of Ahvaz
668 City, Iran. International Journal Of Environmental Research 8(4), 1011-1018

669 De Feo, G., De Gisi, S., 2014. Using MCDA and GIS for hazardous waste landfill siting considering
670 land scarcity for waste disposal. Waste Management 34(11), 2225-2238.
671 <https://doi.org/10.1016/j.wasman.2014.05.028>.

672 Ersoy, H., Bulut, F., Berkun, M., 2013. Landfill site requirements on the rock environment: A case
673 study. Engineering Geology 154, 20-35. <https://doi.org/10.1016/j.enggeo.2012.12.005>.

674 Eskandari, M., Homaei, M., Falamaki, A., 2016. Landfill site selection for municipal solid wastes
675 in mountainous areas with landslide susceptibility. Environmental Science And Pollution Research
676 23(12), 12423-12434. <https://doi.org/10.1007/s11356-016-6459-x>.

677 Eskandari, M., Homaei, M., Mahmodi, S., 2012. An integrated multi criteria approach for landfill
678 siting in a conflicting environmental, economical and socio-cultural area. Waste Management 32(8),
679 1528-1538. <https://doi.org/10.1016/j.wasman.2012.03.014>.

680 Farahbakhsh, A., Forghani, M.A., 2019. Sustainable location and route planning with GIS for waste
681 sorting centers, case study: Kerman, Iran. Waste Management & Research 37(3), 287-300.
682 <https://doi.org/10.1177/0734242x18815950>.

683 Hamzeh, M., Abbaspour, R.A., Davalou, R., 2015. Raster-based outranking method: a new approach
684 for municipal solid waste landfill (MSW) siting. Environmental Science And Pollution Research
685 22(16), 12511-12524. <https://doi.org/10.1007/s11356-015-4485-8>.

686 Han, Z., Ye, C., Zhang, Y., Dan, Z., Zou, Z., Liu, D., Shi, G., 2019. Characteristics and management
687 modes of domestic waste in rural areas of developing countries: a case study of China.
688 Environmental Science And Pollution Research 26(9), 8485-8501. [https://doi.org/10.1007/s11356-](https://doi.org/10.1007/s11356-019-04289-w)
689 [019-04289-w](https://doi.org/10.1007/s11356-019-04289-w).

690 Hanine, M., Boutkhoul, O., Tikniouine, A., Agouti, T., 2016. Comparison of fuzzy AHP and fuzzy
691 TODIM methods for landfill location selection. Springerplus 5. [https://doi.org/10.1186/s40064-016-](https://doi.org/10.1186/s40064-016-2131-7)
692 [2131-7](https://doi.org/10.1186/s40064-016-2131-7).

693 Hoo, P.Y., Hashim, H., Ho, W.S., 2018. Opportunities and challenges: Landfill gas to biomethane
694 injection into natural gas distribution grid through pipeline. Journal Of Cleaner Production 175,
695 409-419. <https://doi.org/10.1016/j.jclepro.2017.11.193>.

696 Huang, S., Feng, Q., Lu, Z., Wen, X., Deo, R.C., 2017. Trend Analysis of Water Poverty Index for

697 Assessment of Water Stress and Water Management Polices: A Case Study in the Hexi Corridor,
698 China. Sustainability 9(5). <https://doi.org/10.3390/su9050756>.

699 GBGMHEGEI, 2015. Gansu Bureau of Geology and Mineral Hydrogeology Engineering
700 Geological Exploration Institute (China). <http://www.gssgy.com/> (Accessed 11 December 2019).

701 GEA, 2015. Gansu Earthquake Agency online portal (China). <http://www.gsdzj.gov.cn/> (Accessed
702 12 December 2019).

703 GESB, 2009. Gansu Environmental Statistics Bulletin (China). <http://sthj.gansu.gov.cn/> (Accessed
704 15 December 2019).

705 GFGB, 2015. Gansu Forestry and Grass Bureau (China). <http://lycy.gansu.gov.cn/> (Accessed 25
706 December 2019).

707 GWRD, 2019. Gansu Water Resources Department (China). <http://slt.gansu.gov.cn/> (Accessed 18
708 December 2019).

709 Kamdar, I., Ali, S., Bennui, A., Techato, K., Jutidamrongphan, W., 2019. Municipal solid waste
710 landfill siting using an integrated GIS-AHP approach: A case study from Songkhla, Thailand.
711 Resources Conservation And Recycling 149, 220-235.
712 <https://doi.org/10.1016/j.resconrec.2019.05.027>.

713 Kara, C., Doratli, N., 2012. Application of GIS/AHP in siting sanitary landfill: a case study in
714 Northern Cyprus. Waste Management & Research 30(9), 966-980.
715 <https://doi.org/10.1177/0734242x12453975>.

716 Karakus, C.B., Demiroglu, D., Coban, A., Ulutas, A., 2020. Evaluation of GIS-based multi-criteria
717 decision-making methods for sanitary landfill site selection: the case of Sivas city, Turkey. Journal
718 Of Material Cycles And Waste Management 22(1), 254-272. [https://doi.org/10.1007/s10163-019-](https://doi.org/10.1007/s10163-019-00935-0)
719 [00935-0](https://doi.org/10.1007/s10163-019-00935-0).

720 Karimi, N., Richter, A., Ng, K.T.W., 2020. Siting and ranking municipal landfill sites in regional
721 scale using nighttime satellite imagery. Journal Of Environmental Management 256.
722 <https://doi.org/10.1016/j.jenvman.2019.109942>.

723 Khan, M.M.-U.-H., Vaezi, M., Kumar, A., 2018. Optimal siting of solid waste-to-value-added
724 facilities through a GIS-based assessment. Science Of the Total Environment 610, 1065-1075.
725 <https://doi.org/10.1016/j.scitotenv.2017.08.169>.

726 Lima, R.M., Santos, A.H.M., Pereira, C.R.S., Flauzino, B.K., Pereira, A.C.O.S., Nogueira, F.J.H.,
727 Valverde, J.A.R., 2018. Spatially distributed potential of landfill biogas production and electric
728 power generation in Brazil. Waste Management 74, 323-334.
729 <https://doi.org/10.1016/j.wasman.2017.12.011>.

730 Liu, H.-C., You, J.-X., Chen, Y.-Z., Fan, X.-J., 2014. Site selection in municipal solid waste
731 management with extended VIKOR method under fuzzy environment. Environmental Earth
732 Sciences 72(10), 4179-4189. <https://doi.org/10.1007/s12665-014-3314-6>.

733 Luo, H., Hu, H., Zhang, M., Zhang, J., 2018. Current Status and Development Trend of Municipal
734 Solid Waste Treatment Technology. Pollution prevention technology 31(03), 22-25.(In Chinese)

735 MODIS, 2018. MODIS (China). <https://modis.gsfc.nasa.gov/> (Accessed 20 December 2019).

736 Motlagh, Z.K., Sayadi, M.H., 2015. Siting MSW landfills using MCE methodology in GIS
737 environment (Case study: Birjand plain, Iran). *Waste Management* 46, 322-337.
738 <https://doi.org/10.1016/j.wasman.2015.08.013>.

739 NCSGI, 2015. National Catalogue Service for Geographic Information(China). <https://webmap.cn/>
740 (Accessed 22 December 2019).

741 NSFTOS, 2017. National Standard Full Text Open System (China).
742 <http://openstd.samr.gov.cn/bzgk/gb/> (Accessed 20 February 2020).

743 Osra, F.A., Kajjumba, G.W., 2020. Landfill site selection in Makkah using geographic information
744 system and analytical hierarchy process. *Waste Management & Research* 38(3), 245-253.
745 <https://doi.org/10.1177/0734242x19833153>.

746 Peng, W., Pivato, A., Lavagnolo, M.C., Raga, R., 2018. Digestate application in landfill bioreactors
747 to remove nitrogen of old landfill leachate. *Waste Management* 74, 335-346.
748 <https://doi.org/10.1016/j.wasman.2018.01.010>.

749 Przydatek, G., Kanownik, W., 2019. Impact of small municipal solid waste landfill on groundwater
750 quality. *Environmental Monitoring And Assessment* 191(3). [https://doi.org/10.1007/s10661-019-](https://doi.org/10.1007/s10661-019-7279-5)
751 [7279-5](https://doi.org/10.1007/s10661-019-7279-5).

752 RESDC, 2015. Resource and Environmental Science and Data Center, Chinese Academy of
753 Sciences (China). <http://www.resdc.cn/> (Accessed 28 December 2019).

754 Rezaeisabzevar, Y., Bazargan, A., Zohourian, B., 2020. Landfill site selection using multi criteria

755 decision making: Influential factors for comparing locations. J. Environ. Sci. 93, 170-184.
756 <https://doi.org/10.1016/j.jes.2020.02.030>.

757 Sener, S., Sener, E., Karaguzel, R., 2011. Solid waste disposal site selection with GIS and AHP
758 methodology: a case study in Senirkent-Uluborlu (Isparta) Basin, Turkey. Environmental
759 Monitoring And Assessment 173(1-4), 533-554. <https://doi.org/10.1007/s10661-010-1403-x>.

760 Sener, S., Sener, E., Nas, B., Karaguzel, R., 2010. Combining AHP with GIS for landfill site
761 selection: A case study in the Lake Beysehir catchment area (Konya, Turkey). Waste Management
762 30(11), 2037-2046. <https://doi.org/10.1016/j.wasman.2010.05.024>.

763 Soltani, A., Hewage, K., Reza, B., Sadiq, R., 2015. Multiple stakeholders in multi-criteria decision-
764 making in the context of Municipal Solid Waste Management: A review. Waste Management 35,
765 318-328. <https://doi.org/10.1016/j.wasman.2014.09.010>.

766 Soroudi, M., Omrani, G., Moataar, F., Jozi, S.A., 2018. A comprehensive multi-criteria decision
767 making-based land capability assessment for municipal solid waste landfill siting. Environmental
768 Science And Pollution Research 25(28), 27877-27889. <https://doi.org/10.1007/s11356-018-2765-9>.

769 Spigolon, L.M.G., Giannotti, M., Larocca, A.P., Russo, M.A.T., Souza, N.d.C., 2018. Landfill siting
770 based on optimisation, multiple decision analysis, and geographic information system analyses.
771 Waste Management & Research 36(7), 606-615. <https://doi.org/10.1177/0734242x18773538>.

772 Sureshkumar, M., Sivakumar, R., Nagarajan, M., 2017. SELECTION OF ALTERNATIVE
773 LANDFILL SITE IN KANCHIPURAM, INDIA BY USING GIS AND MULTICRITERIA
774 DECISION ANALYSIS. Applied Ecology And Environmental Research 15(1), 627-636.

775 https://doi.org/10.15666/aeer/1501_627636.

776 Torabi-Kaveh, M., Babazadeh, R., Mohammadi, S.D., Zaresefat, M., 2016. Landfill site selection
777 using combination of GIS and fuzzy AHP, a case study: Iranshahr, Iran. Waste Management &
778 Research 34(5), 438-448. <https://doi.org/10.1177/0734242x16633777>.

779 Turcott Cervantes, D.E., Lopez Martinez, A., Cuartas Hernandez, M., Lobo Garcia de Cortazar, A.,
780 2018. Using indicators as a tool to evaluate municipal solid waste management: A critical review.
781 Waste Management 80, 51-63. <https://doi.org/10.1016/j.wasman.2018.08.046>.

782 USGS, 2015. United States Geological Survey (US). <https://earthexplorer.usgs.gov/> (Accessed 26
783 December 2019).

784 Uyan, M., 2014. MSW landfill site selection by combining AHP with GIS for Konya, Turkey.
785 Environmental Earth Sciences 71(4), 1629-1639. <https://doi.org/10.1007/s12665-013-2567-9>.

786 Vaverkova, M.D., Adamcova, D., Radziemska, M., Voberkova, S., Mazur, Z., Zloch, J., 2018.
787 Assessment and Evaluation of Heavy Metals Removal from Landfill Leachate by Pleurotus
788 ostreatus. Waste And Biomass Valorization 9(3), 503-511. [https://doi.org/10.1007/s12649-017-](https://doi.org/10.1007/s12649-017-0015-x)
789 [0015-x](https://doi.org/10.1007/s12649-017-0015-x).

790 Williams, M., Longstaff, B., Buchanan, C., Llanso, R., Dennison, W., 2009. Development and
791 evaluation of a spatially-explicit index of Chesapeake Bay health. Marine Pollution Bulletin 59(1-
792 3), 14-25. <https://doi.org/10.1016/j.marpolbul.2008.11.018>.

793 Yousefi, H., Javadzadeh, Z., Noorollahi, Y., Yousefi-Sahzabi, A., 2018. Landfill Site Selection Using
794 a Multi-Criteria Decision-Making Method: A Case Study of the Salafcheghan Special Economic

- 795 Zone, Iran. Sustainability 10(4). <https://doi.org/10.3390/su10041107>.
- 796 Zhang, T., Shi, J., Qian, X., Ai, Y., 2019. Temperature and Gas Pressure Monitoring and Leachate
797 Pumping Tests in a Newly Filled MSW Layer of a Landfill. International Journal Of Environmental
798 Research 13(1), 1-19. <https://doi.org/10.1007/s41742-018-0157-0>.
- 799 Zhang, Z., Dong, Z., Li, J., Qian, G., Jiang, C., 2016. Implications of surface properties for dust
800 emission from gravel deserts (gobis) in the Hexi Corridor. Geoderma 268, 69-77.
801 <https://doi.org/10.1016/j.geoderma.2016.01.011>.

Figures

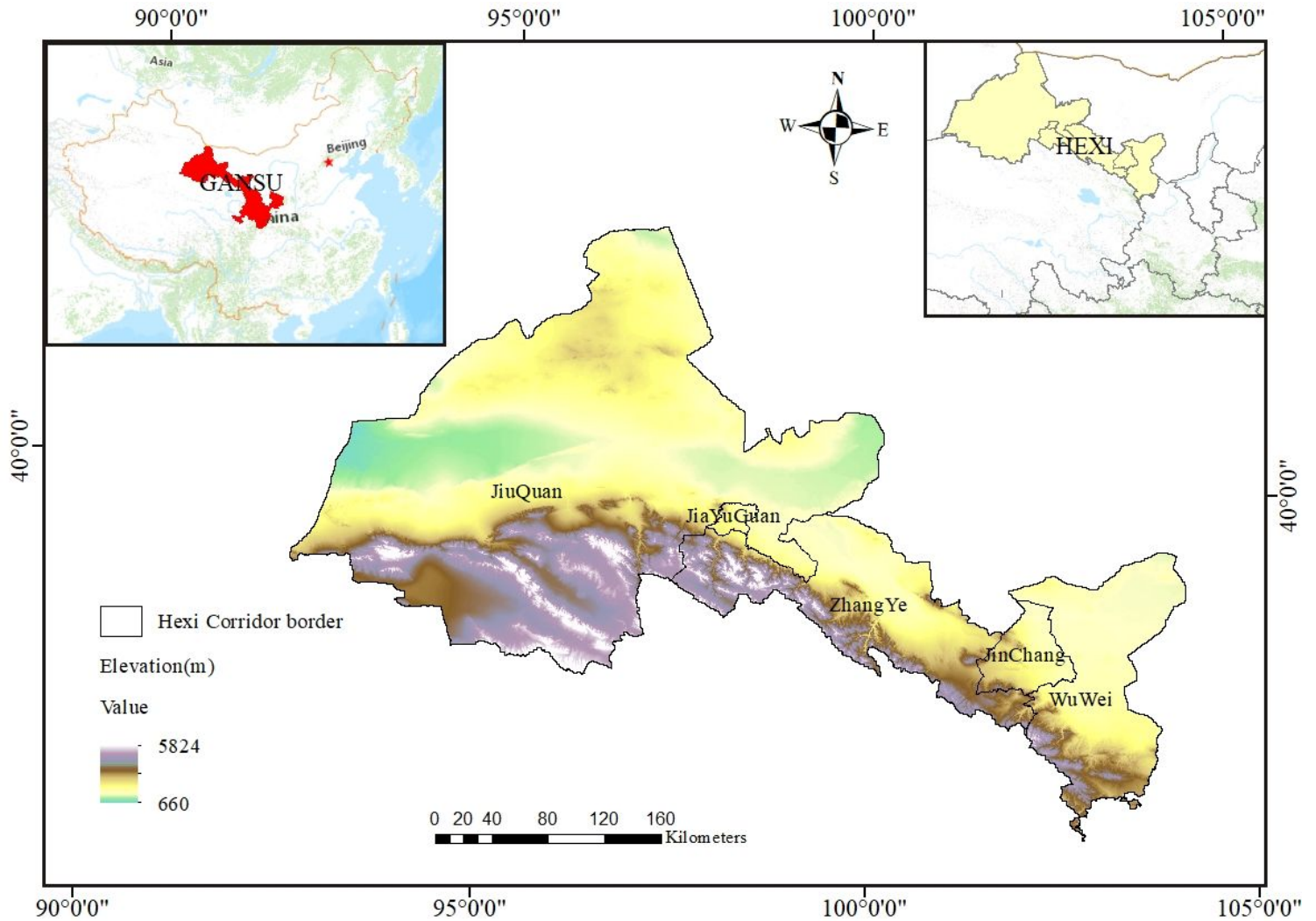


Figure 1

Elevation of the study region. The Hexi Corridor includes five cities (Jiuquan, Jiayuguan, Zhangye, Jinchang, Wuwei), and twenty counties (districts), with a total area of 2.7×10^5 km². Elevation data is from the USGS - SRTM dataset, which provides elevation data at a 30-meter resolution. The elevation of the study area ranged from 660 to 5842 meters. Note: The designations employed and the presentation of the material on this map do not imply the expression of any opinion whatsoever on the part of Research Square concerning the legal status of any country, territory, city or area or of its authorities, or concerning the delimitation of its frontiers or boundaries. This map has been provided by the authors.

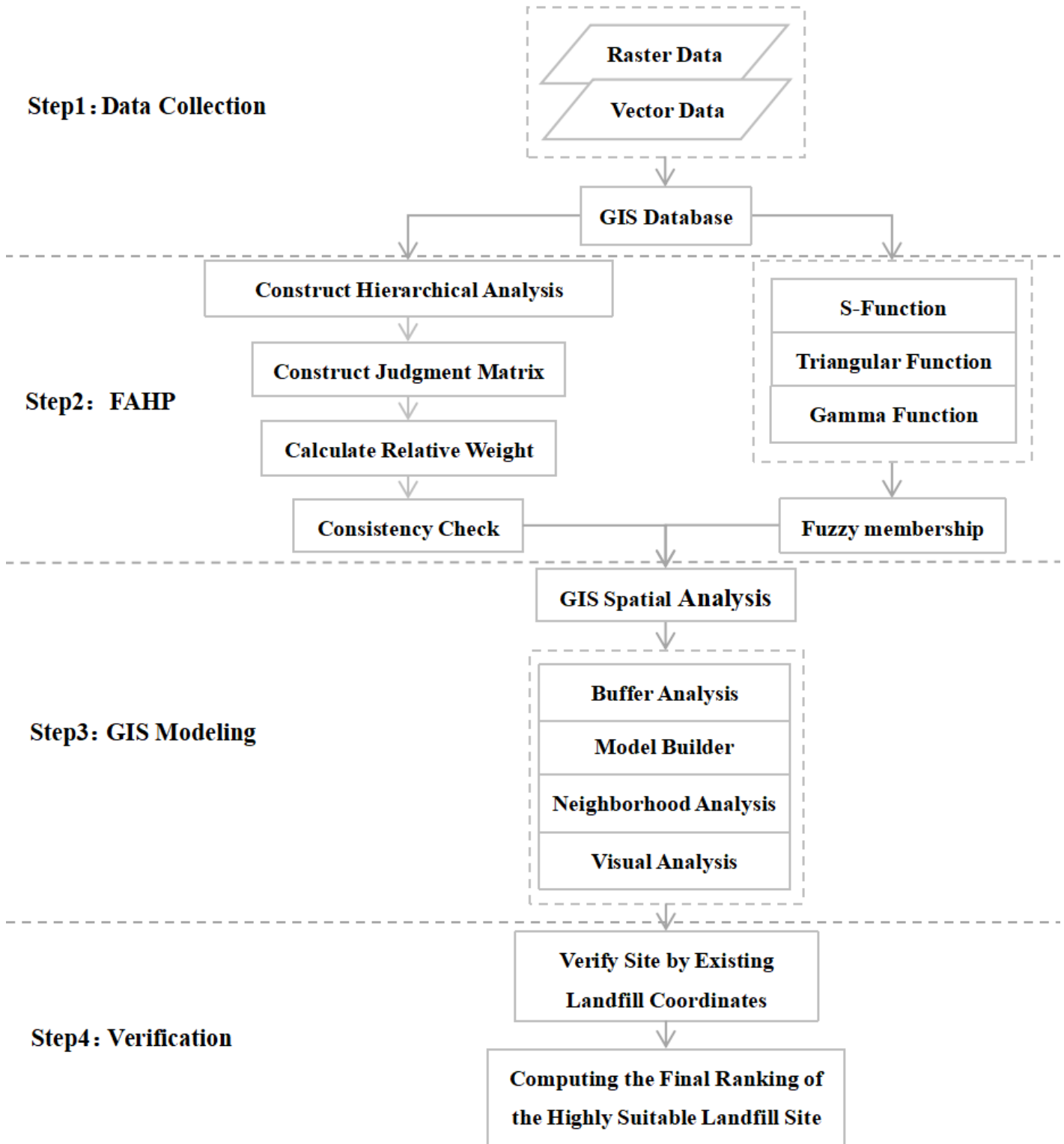


Figure 2

Method framework chart including the four main steps: Data Collection, FAHP, GIS Modeling, and Verification.

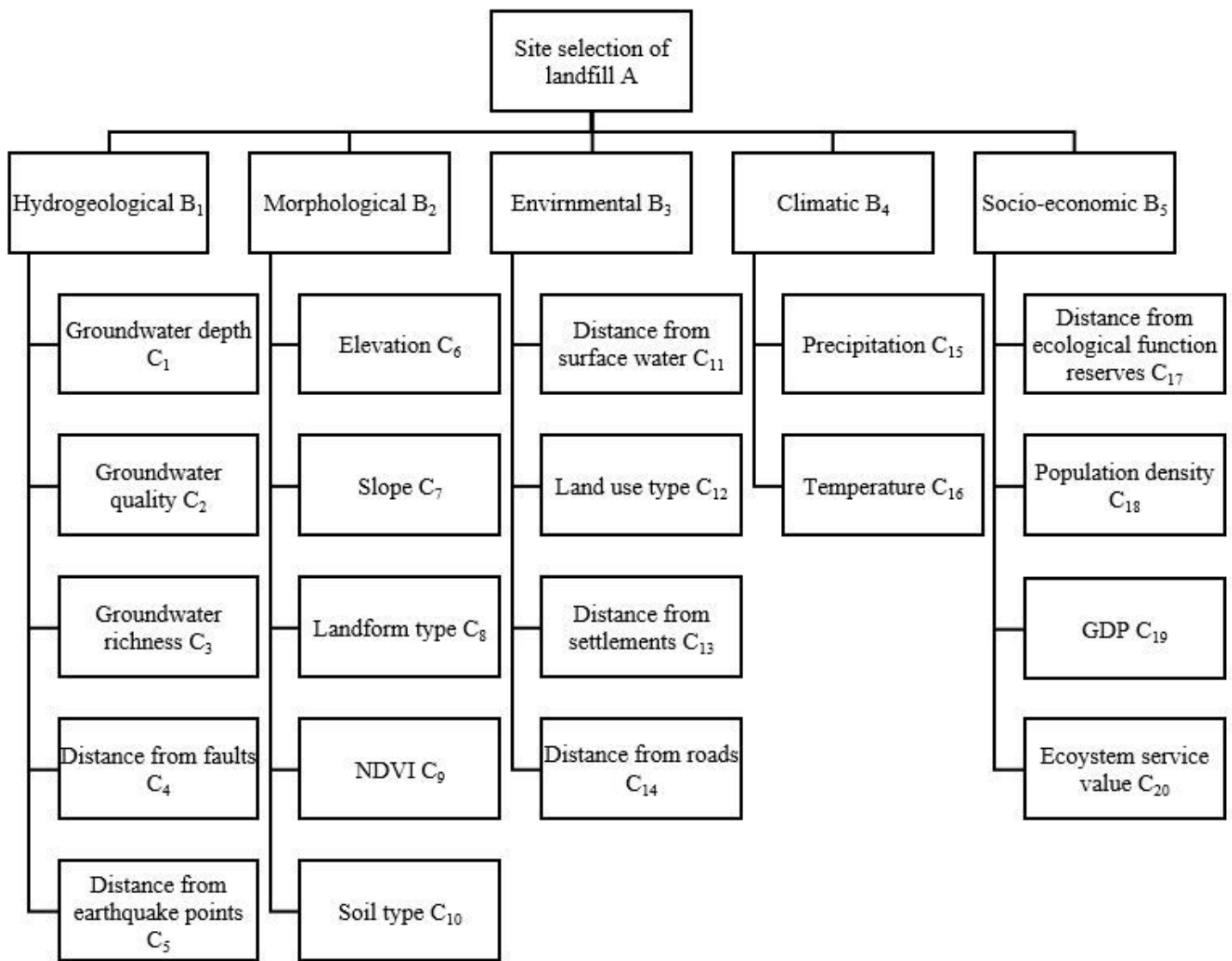


Figure 3

The hierarchical analysis structure is comprised of three layers (decision, primary, and secondary evaluation factor layers). Decision layer A is the site selection of landfill, primary layer B contains five criteria, secondary layer C includes 20 sub-criteria.

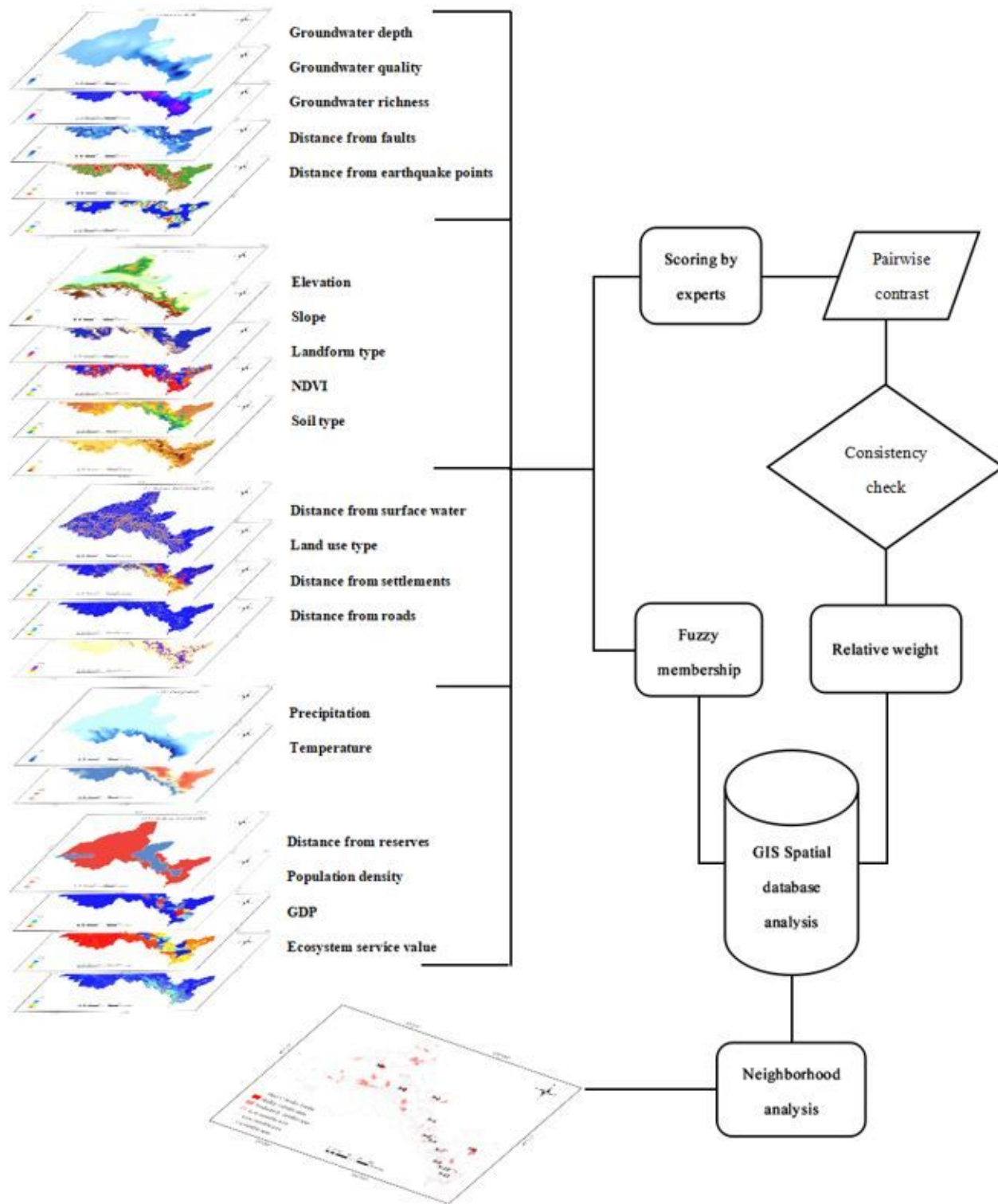


Figure 4

Flow chart of LSS modeling, which includes 20 normalized layers of criteria. GIS spatial analysis was used to calculate its weight and fuzzy membership degree, and obtain the LSSR.

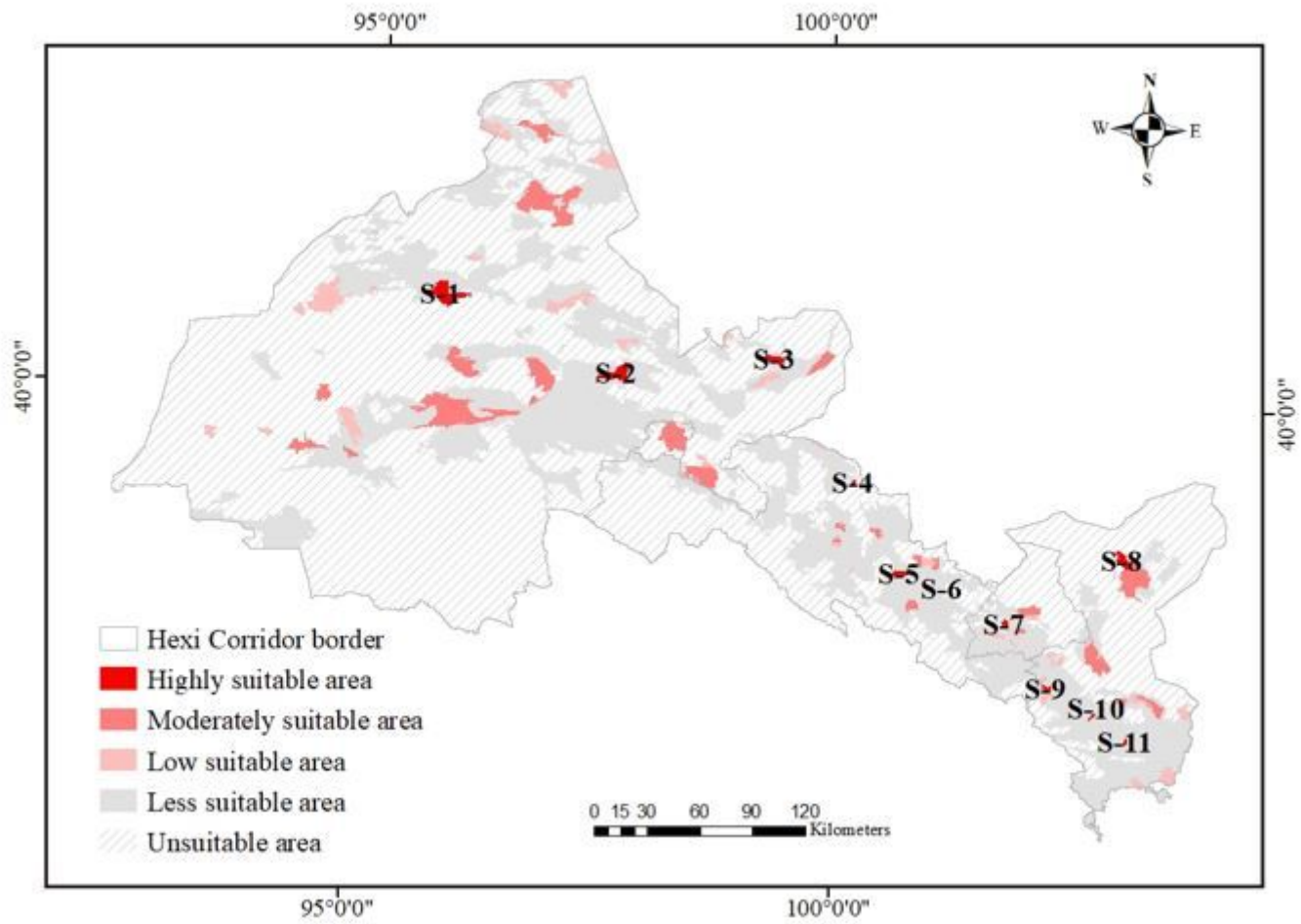


Figure 5

Site selection of MSW landfills in Hexi Corridor. The LSSR are graded according to color brightness. Brighter reds indicate better suitability, gray indicates less suitability, and the line fill indicates the unsuitable. A total of 11 candidate sites were selected in the Hexi Corridor. Note: The designations employed and the presentation of the material on this map do not imply the expression of any opinion whatsoever on the part of Research Square concerning the legal status of any country, territory, city or area or of its authorities, or concerning the delimitation of its frontiers or boundaries. This map has been provided by the authors.

Supplementary Files

This is a list of supplementary files associated with this preprint. Click to download.

- [supplementaryfiles.docx](#)